

Accepted Manuscript

Late Paleocene pipe swarm in the Great South – Canterbury Basin (New Zealand)

Claudia Bertoni, Yuqian (Philomena) Gan, Matteo Paganoni, Jan Mayer, Joe Cartwright, Joe Martin, Pieter Van Rensbergen, Alexander Wunderlich, Alan Clare



PII: S0264-8172(19)30244-2

DOI: <https://doi.org/10.1016/j.marpetgeo.2019.05.039>

Reference: JMPG 3859

To appear in: *Marine and Petroleum Geology*

Received Date: 17 December 2018

Revised Date: 20 April 2019

Accepted Date: 30 May 2019

Please cite this article as: Bertoni, C., Gan, Y.(P.), Paganoni, M., Mayer, J., Cartwright, J., Martin, J., Van Rensbergen, P., Wunderlich, A., Clare, A., Late Paleocene pipe swarm in the Great South – Canterbury Basin (New Zealand), *Marine and Petroleum Geology* (2019), doi: <https://doi.org/10.1016/j.marpetgeo.2019.05.039>.

This is a PDF file of an unedited manuscript that has been accepted for publication. As a service to our customers we are providing this early version of the manuscript. The manuscript will undergo copyediting, typesetting, and review of the resulting proof before it is published in its final form. Please note that during the production process errors may be discovered which could affect the content, and all legal disclaimers that apply to the journal pertain.

Late Paleocene pipe swarm in the Great South – Canterbury Basin (New Zealand)

Claudia Bertoni¹, Yuqian (Philomena) Gan², Matteo Paganoni^{1}, Jan Mayer³, Joe Cartwright¹, Joe Martin⁴, Pieter Van Rensbergen⁵, Alexander Wunderlich³, Alan Clare³*

1-Department of Earth Sciences, University of Oxford, South Parks Rd, Oxford OX1 3AN United Kingdom

2-University of Texas at Austin, Jackson School of Geosciences, 2305 Speedway Stop C1160, Austin, TX 78712-1692

3- OMV New Zealand Ltd, 100 Willis Street, Wellington 6011, New Zealand

4-Shell Exploration & Production Company, 150 North Dairy Ashford, Houston, TX 77079, USA

5- Shell International Global Solution, Rijswijk, The Netherlands.

**Now at Shell International Global Solution, Rijswijk, The Netherlands.*

ABSTRACT

We have identified a deeply buried fluid escape pipe province in Cretaceous - late Paleocene sediments of the Great South–Canterbury Basin (NZ). The seismic observations and interpretations point to an unusually vast fossil system of pipes. These features are exceptional in number (>2000 edifices) and appear to have formed from a common root zone. The areal extent of the analysed pipe system (2500 km²) is among the largest systems of fluid expulsion features ever observed in three-dimensional seismic data.

The unclustered distribution of the pipes suggests no specific link to faults or buried sedimentary features and, at their maximum vertical development, the pipes are equally distributed above depocentres or structural highs. The majority of pipes terminate at two discrete levels in the late Paleocene. Based on the geometrical relationship of the pipe edifices to the overburden, and the basinal setting of the hosting units, we interpret these horizons as representing the seabed at the time of pipe formation. This interpretation allows us to date the timing of pipe formation as prominently late Paleocene. We envisage that the pipes originated during discrete episodes of fluid venting in this time interval, disrupting the typical progressive basinal compaction-driven pore fluid expulsion.

The pipes are associated with biogenic gas expulsion. We discuss their triggers, mechanical processes, and global significance for understanding fluid flow processes in sedimentary basins.

Creation of the initial overpressure could be related to in situ biogenic gas generation in the stratigraphic interval coincident with the root zone of the pipes. We hypothesise that the main episode of gas release and pipe formation was associated with a sea-level fall during the contemporaneous late Paleocene Carbon Isotope Maximum.

This case study shows a unique example of a preserved Paleogene fluid migration system and highlights how the observation and the interpretation of massive fossil systems of fluid-escape features provides invaluable information in terms of overpressure generation and basin fluid expulsion history.

KEYWORDS

Paleocene, pipes, fluid expulsion, biogenic gas, Canterbury Basin, Great South Basin, New Zealand

INTRODUCTION

Fluid-escape pipes provide evidence of anomalous, highly focused pore fluid expulsion in sedimentary basins, in contrast to standard compaction-driven pore-water release. Pipes are generally found in the upper kilometre of the sediment column, in highly layered, clay-dominated marine sedimentary successions, typically of Neogene age (see Cartwright and Santamarina, 2015 and references therein). Alignments and clustering along geological features such as faults, salt or mud diapirs, channels, gas hydrates accumulations are common (e.g. Gay *et al.*, 2007; Løseth *et al.*, 2009; Moss and Cartwright, 2010; Bünz *et al.*, 2012; Maia *et al.*, 2016; Paganoni *et al.*, 2018), and can help identify the mechanisms involved in pipe formation, the fluids feeding the pipes, as well as the root zones of such features. The upwards terminations of pipes can incorporate pockmarks, mounds and other seafloor or paleo-seafloor features. Identifying this termination allows constraining the timing of pipe formation, and understanding their relation to the basin history (e.g. Plaza-Faverola *et al.*, 2011).

The identification, in seismic data, of cross-stratal fluid expulsion features associated with a focused fluid flow can often be directly related to discrete events associated with high fluid fluxes and the release of overpressure. Such events are most commonly triggered by tectonic, climatic or eustatic changes (Andresen and Huuse, 2011; Plaza-Faverola *et al.*, 2011 and 2015; Riboulot *et al.*, 2013 and 2014). Therefore, the analysis of fluid escape pipes can provide fundamental information on the timing and source of overpressures, as well as the scale of the fluid expulsion event. This type of analysis has been traditionally performed in offshore

environments, where the data allow fine-scale resolution of vertical fluid migration pathways (Judd and Hovland, 2007).

The fluids involved in the genesis of fluid-escape pipes include overpressured pore waters, shallow microbial methane, thermogenic hydrocarbons leaking from deeper reservoirs, mud slurry, as well as diagenetic fluids expelled owing to mechanical compaction, chemical compaction, as well as dissolution (Sager *et al.*, 2003; Stewart and Davies, 2006; Hustoft *et al.*, 2007; Kim *et al.*, 2012; Sun *et al.*, 2012; Bertoni *et al.*, 2013; Leduc *et al.*, 2013; Somoza *et al.*, 2014; Paganoni *et al.*, 2018). The migration of such fluids along pipe-like conduits can further result in the accumulation of both gas hydrates and authigenic minerals, as well as in the formation of microbial mats and chemosynthetic communities at the seafloor (Roberts *et al.*, 2006; Paull *et al.*, 2008; Ho *et al.*, 2012; Matsumoto *et al.*, 2017). While the record of a limited cluster of pipes can only hold information on the local behaviour of fluids in the subsurface, the presence of large pipe provinces, composed of hundreds to thousands of single edifices and developed over tens to hundreds of square kilometres, is potentially very significant for the understanding of regional dynamics in sedimentary basins.

Excellent case studies on vast pipes provinces with recent or present-day upwards terminations (i.e. at the seafloor and/or in the shallow overburden) have been presented by Hustoft *et al.* (2010), Moss and Cartwright (2010), Løseth *et al.* (2011), Plaza-Faverola *et al.* (2011), Kang *et al.* (2016), Maia *et al.* (2016) and Kramer *et al.* (2017). Examples of deeply buried, large pipe provinces are more rarely observed (e.g. Maestrelli *et al.*, 2017). In Norway offshore, buried fluid flow features associated with hydrothermal-related Paleogene gas expulsion have been reported (e.g., Iyer *et al.*, 2017). However, normally the data limitations present a challenge to the interpretation of these large provinces buried beyond the first few 100s of metres of overburden, as the detection of pipes is strongly dependant on the vertical and lateral resolution of the subsurface (Cartwright and Santamarina, 2015).

Our study is based on a recently acquired 3D seismic dataset (Figure 1) located in the Great South – Canterbury Basin (GSCB), offshore New Zealand. The high coverage, combined with fine lateral and vertical resolution of the data, allows a detailed morpho-structural interpretation both in section and in plan-view, within the Cretaceous to Recent post-rift section. Previous studies in nearby areas such as the Chatham Rise and the northern part of the Canterbury Basin, highlighted the presence of extensive pockmarks provinces, on the seabed and in relatively shallow buried sediments (Davy *et al.*, 2010; Hillman *et al.*, 2015; Waghorn *et al.*, 2018). These pockmarks have been interpreted as evidence of hydrate dissociation events related to

Pleistocene glacial cycles, groundwater fluid flow associated with bottom currents, and enhanced fluid flow from deep sources. To date, older basinwide focused fluid flow events are unreported in the area.

In this study, we document more than 2000 small-scale circular and positive relief structures occurring in a laterally widespread but vertically limited region of the GSCB. These structures represent an acoustic disruption to the standard configuration of deep-water hemipelagic reflections. These features are hosted in late Cretaceous-early Cenozoic sediments. Their overall morphology is columnar and layer-bound, between the late Cretaceous and late Paleocene horizons. We analyse this extensive sample of columnar structures and interpret them as the largest buried field of fluid escape pipes observed in pre-Quaternary sediments worldwide.

We propose a series of hypotheses for the genesis of the pipes and analyse the potential link to tectonic, hydrological, climatic, as well as hydrocarbon generation events in the basin. Ultimately, this case study aims to add to the knowledge of the fluid flow system of the GSCB, and opens the discussion on the applicability of using pipe fields as indicators of large-scale geological events in worldwide offshore sedimentary basins.

DATASET AND METHODS

The dataset used in this study consists of a 3D seismic survey (Tawhaki-Rigel 3D), 2D seismic profiles and well data located in the GSCB, offshore the New Zealand South Island (Figure 1). The Tawhaki-Rigel 3D seismic survey covers an area of 4880 sq km. It was acquired by Polarcus in late 2011- early 2012 with eight 6 km-long streamers, bin spacing of 6.25x37.5 m, record length of 9.2 s, and a sample interval of 2 ms (and resampled to 4ms in the final processed data). The data was processed for optimal zero phase, and is displayed with SEG standard polarity convention, i.e. an increase in acoustic impedance corresponds to a peak.

The 3D seismic data has been migrated in depth following an horizon-based model and long-distance calibration with the wells. The resultant PSDM processed data show a vertical resolution of approximately 10 m in the first 1-2 s TWT sub-sea which roughly correspond to the Eocene to Recent sediments, while it is 15-20 m in the 2-3 s burial of the sedimentary column, i.e. the approximate extent of the late Cretaceous to Paleocene sequence (the focus of this study). In the absence of direct well calibration, the depth-migrated PSDM data have been considered the most reliable way to interpret depths and produce depth maps of the horizons of interest. Due to 3D migration, features with a lateral extent exceeding the Fresnel zone (ca. 20 m) are expected to be visible (see e.g. Chopra et al., 2006). The depth-migrated time data are

instead routinely considered the most reliable data to produce attribute maps, such as RMS (root mean square) amplitudes and variance extractions and time slices, which highlight in considerable detail fine discontinuities in the data (see e.g. Chopra and Marfurt, 2007). Mapping has been undertaken using standard seismic stratigraphic techniques, in the Schlumberger Petrel software, and using autotracking to produce areally complete horizon surfaces.

We also used spatial alignment analysis to highlight areal patterns and to understand the statistical distribution of the pipes. This method was implemented by considering the average nearest neighbour univariate spatial autocorrelation statistical method (see Maia *et al.*, 2016). The resulting data were then used to produce a rose diagram which represents the distribution of the alignments of the pipes. This was measured by counting the number of pipes found within a search window of length l and width w , rotating at each pipe n with angle step θ . The alignment selected for each pipe n is simply based on the largest number of pipes found in a complete search (0-360 degrees).

2D seismic lines from the surveys OMV08-OMV10 and DUN06 were used for long-distance well correlation to the 3D seismic data (Figure 1). The seismic dataset covers a stratigraphic succession from Late Paleozoic to recent sediments, in the GSCB (Figure 1) (Uruski and Ilg, 2006; Constable *et al.*, 2013). The wells used for the long-distance stratigraphic tie are located in the near-shelfal and slope area on the western flank of the GSCB, and provide long-distance ties to the 3D seismic surveys through the 2D seismic lines (Figures 1 & 2). The well tie, where the most representative wells are the Tara-1 and Toroa-1, allows us to constrain the stratigraphic units and the depositional context in the interval of interest in the more basinward study area.

The nomenclature of the seismic horizons has been largely based on the sequence stratigraphic framework produced by Constable *et al.* (2013), with the addition of further horizons, and updated for more recent studies (OMV internal report) (Figure 2) where needed. In order to constrain the possible changes of sediment properties within the study interval, we correlated the markers from the Tara-1 and Toroa-1 wells on the shelf to their equivalents in the basin. We interpreted the lithology of these intervals based on seismic stratigraphic observations (Constable *et al.*, 2013), and by analogy with the data published on the Caravel-1 well, drilled in the Canterbury basin in a more basinal position, paleogeographically similar to the basinal area of the Great South Basin (Blanke, 2015).

GEOLOGICAL AND SEISMIC STRATIGRAPHIC SETTING

The area of interest is underlain by a pre-rift sequence of Late Paleozoic to Jurassic/Cretaceous age, composed by the Murihuku, Dun Mountain- Maitai and Caples terranes (Figure 1) (Bache *et al.*, 2014; Uruski, 2015). A syn-rift sedimentary series records the break-up of Gondwana, which occurred in the area most probably from Early Cretaceous, around 112 Ma, coinciding with the opening of the Gippsland Basin in Australia (Bache *et al.*, 2014; Internal OMV Reports). This structural configuration is reflected in deep NE-SW trending fault lineaments, bounding local Cretaceous depocentres. Some of these faults have been later reactivated and inverted (Figure 2). This unit is arranged into asymmetric, half-graben wedges and bounded at the top by horizon K50 (Figures 3 and 4).

The early syn-rift series is composed of lacustrine, alluvial and fluvial deposits, and it is overlain by transgressive marine sands and fine-grained siliciclastic sediments (Cook *et al.*, 1999). In the study area, the syn-rift wedges are composed of generally discontinuous, high- to mid-amplitude reflections, onlapping the flanks of the intervening horsts (Figure 3). The syn-rift series hosts the main source rock for petroleum generation in the GSCB, which is thought to be non-marine, coaly sediments of the Hoiho Group (Late Cretaceous, see Pearson, 1998; Cook *et al.*, 1999; Sahoo *et al.*, 2014), based on the findings of wells drilled in the Great South and Canterbury Basin. Coals within the Hoiho Group are located at horizons K20 (and K40, not shown in this study) in the syn-rift series. In between these horizons coaly organic material was most likely dispersed due to higher background sedimentation (Figure 3)(see Sahoo *et al.*, 2014 and 2015). The results from the most recently drilled well in the contiguous deep-water Canterbury basin show potential for an additional late Cretaceous marine source rock, which is associated to a maximum flooding surface (Blanke, 2015). Additionally, oil shows sourced from a marine source rock have been encountered in the Paleocene section in the Kawau-1A well, south of the study area (Hunt International, 1977).

The syn-rift unit is overlain by a Late Cretaceous to Oligocene post-rift series (Figure 1). This series is bounded at the base by horizon K50, and at the top by horizon T70 (Figure 2). The seismic facies of the post-rift series is generally characterised by low to moderate amplitude, parallel and relatively continuous seismic reflections (Figures 1 and 3), an acoustic expression that is typical of hemipelagic and fine-grained marine sediments. This layered sequence, in the north-western part of the study area, hosts a series of hydrocarbon-related amplitude anomalies (Bertoni *et al.*, 2018).

A marked change in seismic character occurs in the eastern part of the basin, which is specifically the focus of this study. In this area, the interval between the K50 and T50 horizons

(Figure 3) exhibits decreased thickness. The unit is seismically characterised by parallel reflections with a consistently high-amplitude character (Figure 4). The change in thickness and seismic character could be related to lithological factors, and possibly controlled by differential vertical tectonic movements and/or differential compaction in the two parts of the basin. The change in thickness, as well as the observed undulating seismic facies, could also be related to differential advancement of paleo Opal A-CT boundaries (Meadows and Davies, 2008, Morley et al., 2017). Based on data available, it is not possible to discern among these potential controlling factors.

An important post-rift regional marker is horizon T10, which corresponds to organic-rich marine shales identified in different basins in New Zealand either as the Tartan or Waipawa formation (Figures 1b and 4). These deposits are widely recorded in the Thanetian (late Paleocene, 58.7-55.8) of Eastern New Zealand (Killops et al., 1996; Hollis et al., 2005; Schioler et al 2010; Constable et al., 2013). In the Great South and Canterbury Basin, the Paleocene and Eocene were times of significant climatic and local tectonic changes, including a series of Paleogene thermal minima, and climatic events at the end of Paleocene and beginning of Eocene (Paleocene-Eocene Thermal Maximum (PETM) - late Paleocene carbon isotope maximum (PCIM, 59-56 Ma) - initial Eocene thermal maximum (IETM, 55.5 Ma)), plate tectonic movements and changes in oceanic current patterns (Killops et al., 2000; Hollis et al., 2005 and 2014; Nicolo et al., 2007; Zachos et al., 2008; McInerney and Wing, 2011)

The presence of the T10 organic shales has been related to the PCIM), and they record the influence of globally increased marine productivity, across a subsiding continental margin (Killops et al., 2000; Hollis et al., 2005; Nicolo et al., 2007; Zachos et al., 2008; MacInerney & Wing, 2011). This event is associated with cool, eutrophic conditions that accelerate the rate of carbon burial in many New Zealand sedimentary basins (Killops et al., 2000). The Tartan formation was deposited on a relatively flat and restricted basin floor, and associated to a eustatically driven base level fall, before a latest Paleocene - earliest Eocene transgression (Schioler et al., 2010).

In the Canterbury basin, distal post-rift Paleocene-Eocene sediments drilled from Caravel-1 well (Figure 1) are fine-grained, quartz-rich sediments with high porosity but low permeability (Blanke 2015). These sediments are considered the closest analogue to the late Paleocene-Eocene deposits of the study area. Evidence of silica diagenesis is also found in these deposits.

The top of the post-rift sequence is composed of Oligocene deep-water clastic sediments that record the increased influence of contour currents reworking and have been linked to the opening of the Tasman Strait and reorganization of oceanic currents in the GSCB and in the

wider south-east Pacific area (Lu et al., 2003; 2005). The most recent unit in the study area spans in age from Miocene to Recent and is composed of syn-orogenic deposits, associated with the oblique collision of the Australian and Pacific plates, which led to the formation of the Southern Alps (Hall et al., 2004, OMV report). This tectonic phase created inversion structures in parts of the GSCB, such as around the Tara-1 and Toroa-1 wells (Figure 1 and 2).

DESCRIPTION

The late Cretaceous to Paleocene early post-rift unit in the study area is characterised by layered deep-water clastic or hemipelagic sediments, with a sub-parallel seismic configuration. This laterally continuous layered sequence is locally disrupted by a set of columnar zones characterised by a chaotic-to-transparent seismic character (Figure 4). There is an exceptional number (>2000) of these seismic disturbances across the study area, and they are concentrated in the areas where the overall thickness of the early post rift section thins to less than ca. 450m (Figure 5). We mapped in detail the distribution of these zones, and analysed their geometry and seismic expression, in order to unravel their origin, timing, and significance at the basin scale.

Observations on seismic sections allow to divide the columnar structures into three distinct parts: the 'upper terminus', the 'lower termination' and the connection between them, i.e. the 'conduit', using a terminology that has been previously applied to describe vertical pipe-like features on seismic data (e.g. Cartwright and Santamarina, 2015; Kirkham *et al.*, 2018).

Upper termini

The upper termini are the shallowest expression of the disturbance zones. In the study area, they are characterised by convex upwards morphology and display a positive relief of approximately 30-50 ms (35-55 m) on horizons T00, T10 (late Paleocene), and occasionally, T50 (early-mid Eocene) (Figures 4 and 6). No upper termini are observed below T00. Identifying the stratigraphic position of the upper termini is important because it links them with the point of piercement of the fluid-escape pipe with the present or paleo seabed, expressed as (paleo) seafloor depressions (i.e. pockmarks), or as accumulations of intrusive and extrusive material (i.e. mud volcanoes, hydrate pingoes, and authigenic carbonate mounds). Therefore, with a suitable seismic resolution, the upper terminus of the fluid conduits can reveal the age of the fluid expulsion, as well as the nature of the paleo-seabed expression.

The planform of the upper termini of the columnar structures is best visualised on TWT maps, and horizon-based variance extractions along horizon T07 and T10 (Figure 7 and 8). The overall 3D morphology of the upper termini is mounded (Figure 7), and circular to subcircular in horizontal section, with a diameter of 100 to 300m (Figure 6). The vast majority of the upper termini are located at horizon T00, on which we identified ca. 1400 pipes (Figure 8).

A smaller percentage of the upper termini (ca. 30% of the total number, i.e. 600 pipes) are located at horizon T10. Furthermore, a few examples of upper termini are also located on horizon T50 (Figure 9). The vast predominance of upper termini on horizon T00, compared to horizons T10 and T50, is evident particularly in the areas above the syn-rift depocentres (i.e. the areas of major syn- and post-rift sedimentation), between the two main structural highs (Figure 4 and 6). It should further be considered that the thickness of the T10-T60 sedimentary section decreases significantly over the structural highs, and onlap patterns are observed on the flanks of these structures as a result of differential compaction and, possibly, paleocurrent patterns and sediment redistribution (Figure 4). In these areas of relatively condensed sedimentation, the interpretation of horizons T10 to T50 is challenging, due to both limits of seismic resolution and the further presence of post-T00 discontinuous surfaces. As a consequence, there are some areas where the stratigraphic location of the upper termini of the columnar structures is not clearly resolvable within the sedimentary package.

The overall areal distribution of the columnar structures is best analysed by mapping the location the upper termini on the variance maps extracted along individual horizons. The maximum density of the pipes and their most widespread areal coverage is observed on the variance map extracted along horizon T00 (Figure 8). The SE boundary of the mapped pipe extent is defined by the boundary of the 3D seismic survey. Their NW boundary is irregular, following the salients and embayments of the TWT structural map of horizon T00, and corresponds well with the transition from shelfal to deepwater environments mapped from Paleocene paleobathymetry (Figure 8). Basin environments have been interpreted by means of interpolation of seismic thickness and facies changes of the interval of interest, tied to regional well data (OMV internal report). The distribution of the pipes is also correlated to the areas of the minimum thickness of the K80-T00 interval (Figure 5), with an average cut-off for thicknesses >450 m ca. (~375 ms ca.).

We performed spatial alignment analysis of upper termini of the pipes on horizon T00, by considering the average nearest neighbour univariate spatial autocorrelation statistical method

(see Maia *et al.*, 2016). The resulting Rose diagram shows a widely scattered distribution with no large-scale preferential alignment of the pipes (Figure 8). The rose diagram represents the distribution of the alignments of the pipes. Small-scale clustering is locally found, generally at sub-circular or irregularly elongated depressions on horizon T00, coincident with relative thickness minima of the K80-T00 interval (Figure 8). Overall, the distribution of the pipes shows no relation to structural lineaments (e.g. faults), depositional features (such as channels), and igneous sills.

Root zones

The root zones of columnar structures are the deepest regions where the deformation associated with the acoustic disturbance is observed. On seismic sections, this is identified as the first continuous reflection beneath the stacked vertical zone of discontinuity (see Gay *et al.*, 2012; Cartwright and Santamarina, 2015). We defined as the lower termination the deepest points of the columnar disturbance associated with breaks in reflection continuity. Based on these characteristics, we observed that the vast majority of the root zones are located in the interval K80 to K100 (near Top Cretaceous) (Figures 6 and 9). The root zones are located in proximity to horizon K80 and most likely start at horizon K90, which, however, is not regionally mappable on the seismic data. This event corresponds to a transgressive shale (organic-rich in Caravel-1).

In the study area, the identification of the root zones can be particularly challenging, due to both the limits of seismic resolution at the subsurface depth of these features and potential acoustic artefacts. In general, seismic imaging accuracy decreases with depth and with the decreasing width of the disruption zone observed (Løseth *et al.*, 2011). In the interval below the upper termini, the decrease in frequency and loss of resolution of the seismic data can constitute a potential imaging issue and generate seismic artefacts and spatial bias. Seismic artefacts can result in poor migration of the data, distortion due to velocity pull-up or push-down, low signal to noise ratio, reflected refractions, uncollapsed diffractions and complex multiples (Cartwright and Santamarina, 2015). The signal disruption can be included or propagate beneath the root zones (see Cartwright *et al.*, 2007). In order to address these issues, we interpreted as root zones only the unequivocally clear terminations, represented by the larger columnar features associated with breaks in reflection continuity, or a change in signal disruption which is not consistent with the vertical propagation of a processing artefact (e.g. break in continuity changing downwards to pull-up distortion) (e.g. Figure 6 and 9).

Conduits

The conduits represent the connection between the upper termini and root zones of the columnar disturbance features. Their expression on seismic section is represented by the vertically or sub-vertically stacked breaks in reflection continuity, commonly associated with amplitude attenuation. On seismic sections, the vertical extent of the columnar disturbances varies between 100 and 400 ms ca. (Figure 6, 9 and 10). The vertically most extensive conduits are generally located in the areas above the syn-rift basins, where the K50-T10 sedimentary package is thicker than above the structural highs. The width of the conduits is consistent with the measured widths of the upper termini and root zones previously described, extending laterally for 100 to 300m. The planform of the conduits is particularly clear on horizontal variance time slices, where it appears as sub-circular to sub-elliptical (Figure 11).

Similar to the root zones, the interpretation of the conduits can be challenging, as the visualisation of their lateral margins strongly depends on the presence of anomalous amplitudes at or around the conduit. We, therefore, identified the lateral margins of the conduits by interpreting as conduits only the unequivocally clear breaks in reflection continuity within the larger columnar features (Figure 10b and c), while discarding the vertically or sub-vertically attenuated amplitudes associated with continuous reflections. Overall, the height of the conduits is more pronounced than their lateral extent, defining a h/v aspect ratio of 1:2 to 1:5. Overall, the circular/sub-circular planform associated with the vertical extent of the conduits define a three-dimensional cylindrical morphology.

INTERPRETATION

The columnar structures observed in 3D seismic data are interpreted as fluid-escape pipes on the basis of the following observations, which are typical of such features (see Cartwright and Santamarina, 2015 and references therein): 1) the cylindrical character of the conduit; 2) the disrupted, low frequency and low amplitude internal seismic character of these features which interrupt an otherwise continuous sub-horizontal stratigraphic layering; 3) the strata-bound vertical extent, mostly confined between horizons K80 and T10 and 4) the h/v aspect ratio (<1).

Nature of upper termini and timing of formation

The observed fluid-escape pipes are characterised by a mounded, convex-upward morphology of the upper terminus (Figure 7 and Figure 10b-10d). The nature of the upper pipes termini, if coinciding with the paleo-seafloor at the time of pipe formation, is important in order to identify the genetic process of the pipe, and to pinpoint the timing of pipe genesis with respect to the

geological history of a basin (e.g. Davy *et al.*, 2010; Plaza-Faverola *et al.*, 2011; Riboulot *et al.*, 2014). Pipes are commonly capped by pockmarks, which are seafloor depressions representing the seabed expression of their upper termini (Gay *et al.*, 2007; Bünz *et al.*, 2012).

However, in particular circumstances, pipes have been interpreted as incipient ‘intrusive’ features, where the upper termini represent the shallowest expression of an internal blowout, which evolves into a more diffusive seepage in the lower-most sedimentary section owing to a significant lithological change (i.e. the presence of glaciogenic sediments) (Van Rensbergen *et al.*, 2007). Such intrusive pipes do not have either a seabed expression or well defined upper termini, which are clear features we see for pipes in our dataset. Therefore, the presence of well-defined mounds at the pipe termini in the study area rules out their interpretation as intrusive structures. Furthermore, on several pipes, the immediately overlying reflections show a downlapping or onlapping relationship with the post-T00 overburden (Figure 10), which can be best explained by overlying hemipelagic sediments healing the topography produced by the pipe topography on the seabed at the time of formation. This observation suggests that the onlap/downlap surface represents the seabed at the time of pipe formation; however, the possible effect of differential compaction and seismic tuning could have partially contributed to creating similar reflection configuration.

The observed fluid-escape pipes display mounded upper termini, which is consistently located at horizons T00 and T10, within one seismic loop of each horizon. Examples of mounded or morphologically more irregular terminations at the seafloor have been observed at the top of fluid escape pipes and may be the seismic expression of a constructive edifice generated by diagenetic/extrusive mounds above hydrothermal vents (Hansen *et al.*, 2005; Planke *et al.*, 2005), remobilised sediments (mud/asphalt volcanoes or clay diapirs) (Bouriak *et al.*, 2000; MacDonald *et al.*, 2004; Stewart and Davies, 2006), diagenetic mounds associated with authigenic carbonate precipitation and methane fluxes through gas hydrate stability zones (Talukder *et al.*, 2007; Crutchley *et al.*, 2014), and gas hydrate pingoes (Paull *et al.*, 2007; Serié *et al.*, 2012).

The mounded upper termini of the pipes described in the late Paleocene of the GSCB show no correlation with underlying igneous sills on vertical sections in the seismic data. Furthermore, their spatial distribution does not suggest any alignment that can point to a genetic relationship with underlying sills, as commonly observed in igneous provinces (Planke *et al.*, 2005; Manton, 2015). Therefore, among the possible interpretations, we can exclude their origin as mounds associated to hydrothermal vents.

The hypothesis of a relation between these mounds and fluid venting from a paleo base of gas hydrate stability zone (BGHSZ), and potential subsequent methanogenic carbonate precipitation, can be tested by analysing the burial conditions of the source interval for the fluids generating the pipes. Such a system would imply a root zone which is laterally consistent with the gas hydrate phase boundary, which is controlled by fluid pressure and temperature, and frequently observed to cross-cut stratigraphic reflections and represent the top of a potentially overpressured free gas accumulation (Flemings *et al.*, 2003; Bünnz *et al.*, 2012).

The water depth at the time of deposition of the T00 to T10 horizons, is largely unconstrained in this deep-water portion of the basin. Facies analysis tying regional well data to seismic facies and thicknesses suggests that the depositional environment of the pipe-hosting sediments in the late Paleocene was slope to basin floor. The analysis of the lower pipe termination points has highlighted that the root zone of the pipes, where visible, is consistently located in the Late Cretaceous stratigraphic interval (K80). This argues for a stratigraphically-controlled rather than P-T-controlled (i.e. the base Gas Hydrate Stability zone, GHSZ) source of the remobilised sediments/fluids feeding the pipes from early post-rift Late Cretaceous-early Paleocene sediments. Based on these observations, the genetic link between a base GHSZ and the pipe root zone is unlikely.

For the reasons listed above, the preferred interpretation of the mounded upper termini morphology is interpreted to reflect the presence of a constructive edifice sustained by hydrocarbon gases seepage to the seabed, unrelated to a natural gas hydrate system, or of a clastic extrusive feature, such as a small-scale mud volcano or clay diapir.

The absence of preferential clustering or alignment of pipe distribution in two and three-dimensions rules out a direct genetic link to depositional and structural elements that would result in an inherited preferential alignment, such as observed in pockmarks fields and mounds developed above salt domes, shale-cored anticlines, faults or channels (Gay *et al.*, 2006; Sultan *et al.*, 2011; Serié *et al.*, 2016). Therefore, there is no indication that the fluid vented along the pipes has been focused in a specific structurally- or stratigraphically-controlled zone, but rather points towards a laterally widespread distribution of the escaped fluid.

Regardless of the nature of the mounded upper termini, their stratigraphic location is a clear indication of the timing of pipe formation. Consequently, the location of the upper termini predominantly at horizons T00 and T10 signifies that the mounds and the pipes are of a fossil nature and were formed over a geologic interval coincident with the late Paleocene. The occurrence of a much smaller number of pipes, and of lower areal density, in the early-mid Eocene (T50) indicates the existence of a second phase of pipe formation.

DISCUSSION

The seismic observations and interpretations presented in this study point to an unusually vast fossil system of fluid-escape pipes. These unclustered features are exceptional in number and appear to have formed synchronously from a common root zone. In the paragraphs below, we discuss their geometry, triggers, mechanical processes, and global significance for fluid flow in sedimentary basins.

Mechanical genetic process

The areal extent of the analysed pipe system (2500 km²) is among the largest systems of fluid expulsion features ever observed in three-dimensional seismic data. An analogue system could be that described by Hartwig et al. (2012), in South Africa (Orange Basin). In this case, the authors identified a 2800 km² large pockmark field, stratigraphically limited to the Early Eocene, which slightly postdates the age of the termini of the pipes observed in this study (late Paleocene). Earlier, Andresen et al. (2008) identified a system of paleo-pockmarks in the Danish North Sea, stacked at two different stratigraphic levels (mid-Oligocene and late-Miocene). Similarly, Cole et al. (2000) identified giant craters in early Eocene sediments in the UK North Sea. These three studies all pointed to overpressures associated with petroleum generation as a possible genetic mechanism for these pockmarks. However, none of them imaged the conduits that allowed such fluids to migrate towards the (paleo) seafloor. Thus, this study shows a unique example of a preserved Paleogene fluid migration system.

When comparing the Paleocene pipe province in the area of interest with presently or recently active large-scale fluid expulsion systems, there are a series of examples, in terms of areal extent and conduit geometry, which have been observed in different geological settings and can provide analogues for understanding the overall distribution and triggers of the pipes. Such analogues are:

- (1) Offshore Norway (Hustoft et al., 2010) (i.e. the Nyegga pockmark field), where the pipes root into free gas reservoirs deeper than the present-day base of gas hydrate stability zone (BGHSZ) and breach the seafloor, creating pockmarks. In the same area, Plaza-Faverola et al. (2011) recognised a glaciation-driven episodicity in the events of fluid flow for the last ~200 ka.
- (2) The Dnieper paleo-delta, northwestern Black Sea (Naudts et al., 2006), where almost 2800 gas seeps, associated with pockmarks or other geomorphic features, have been

identified in association with the vertical migration of methane, above the feather edge of hydrate stability, i.e. in the upper slope and on the shelf.

- (3) The NW shelf of Australia (e.g. Yampi Shelf, NE Browse Basin), where chimney-like conduits and associated hydrocarbon-related diagenetic zones have been imaged on 3D seismic and are associated with hydrocarbon leakage from deep reservoirs, as further confirmed by the identification of slicks in the water column (O'Brien et al., 2005).
- (4) The Barents Sea, where massive blow-out craters and mounds, as well as gas flares, have been identified and attributed to a natural gas hydrate system leaking free gas in response to glacial cycles and sourced from an underlying active petroleum system (Andreassen et al., 2017).
- (5) The Dutch Dogger Bank seep area (North Sea), where methane emission sourced from shallow gas pockets through pipe-like conduits, are capable of bypassing the shallow water column (~40 m), up to the atmosphere (Römer et al., 2017).
- (6) The St. Lawrence Estuary (Canada), where the generation of nearly 2000 actively methane-venting pockmarks is considered to be linked to deeper leaky Paleozoic thermogenically-sourced reservoirs, as suggested by seismic imaging and geochemical data (Lavoie *et al.*, 2010).
- (7) The recent eruption of a large pockmark field has been documented by Kramer et al. (2017). The authors suggest a storm wave induced triggering mechanism. Interestingly, in this case study the sea-level change is considered a key factor in triggering the expulsion of fluids and formation of pipes, although in a much shallower water-depth setting compared to the study area.
- (8) A large pockmark field has been reported by Chenrai and Huuse (2017). In this case, porewater expulsion during overburden progradation was pinpointed as the most likely cause of the paleo-pockmarks, due to rapid sediment loading and generation of differential overpressure imposed by clinoform progradation. This peculiar load configuration is although absent in the study area in the GSCB due to its relatively deep water setting and laterally continuous sedimentary load.

In the cases quoted above and other worldwide examples, the generation of fluid-escape pipes has been attributed dominantly to episodes of pore pressure build-up. Such pore pressure increase has been attributed to different causes, including the formation of buoyant hydrocarbon columns, hydrocarbon diagenesis (i.e. fluid expansion), lateral pressure transfer, and reduction in the hydrostatic load in a basin (e.g. because of global sea-level changes or uplift). Such episodes of pore-pressure build-up could be enough to trigger a single- or multi-phase cross-stratal fluid flow through (1) fracturing, (2) capillary invasion, and (3)

fluidisation/liquefaction, with the latter process implying the migration of solid particles and fluids along a cross-stratal pathway. For the three mechanisms described, generation of excess pore pressure overcomes (1) the minimum effective stress and the sediment tensile strength (2) the capillary forces at the pore scale, and (3) the effective vertical stress in the cohesionless host sediment, respectively (cf. Jain and Juanes, 2009; Hustoft *et al.*, 2010; Gay *et al.*, 2012; Cartwright and Santamarina, 2015).

The sediments hosting the observed fluid-escape pipes in the study area are interpreted to be fine-grained and thus characterised, even at the time of pipe formation, by both nm-sized pore throats and a certain amount of tensile strength, as a result of consolidation, cementation, and capillary water forces (in multi-phase systems, i.e. with free gas) (Jain and Juanes, 2009; Nelson, 2009; Mourgues *et al.*, 2011). Both these elements would favour fracturing against the other two mechanisms as the most likely genetic mechanism for the observed fluid-escape pipes, as further argued by many other studies on similar features (Hustoft *et al.*, 2010; Moss and Cartwright, 2010; Maestrelli *et al.*, 2017).

Considering the average actual pipe height (~125-450 m) and a standard decompaction rate of ~20-40% normally used to calculate original thicknesses in fine-grained sediments in the first few hundreds of metres of overburden (cf. Giles *et al.*, 1998), we estimate that the pipes had an original height of between ~150 and 595 m. Assuming seawater and sediment bulk densities, respectively of 1.025 g/cm³ and 1.8-2.0 g/cm³, and original hydrostatic conditions at the root zones, we deduce that the effective vertical stress at the root zones is between 1.1 and 5.92 MPa. Therefore, the amount of excess pore pressure required to generate fractures and trigger the formation of the observed pipes could approach the calculated effective vertical stress plus any sediment tensile strength and would be in the order ~1-6 MPa.

Triggering events

The location of the mounded upper termini of the pipes at the late Paleocene seabed constrain the formation of these edifices to this time interval. This hints that during the late Paleocene, basin-scale processes occurred to trigger the vast fluid escape event that generated the pipes. Considering the stratigraphic setting of the area and the geological history, we discuss five possible mechanisms as potential contributors to overpressure generation close to the fracture gradient and fluid release at the root zones of the analysed pipes: a) gas hydrates dissociation, b) buoyancy-related overpressure owing to the formation of a connected hydrocarbon column, c) fluid expansion due to the generation exsolution/ebullition, or expansion of hydrocarbon fluids, d) lateral and vertical pressure transfer, e) change in temperature, stress and loading conditions.

Natural gas hydrate dissociation has often been invoked as a potential overpressure generation mechanism in shallow sediments (Sultan *et al.*, 2004; Xu and Germanovich, 2006; Holtzman and Juanes, 2011), capable of triggering the vertical migration of free gas towards the seafloor. In this scenario, the root zones of the pipe would match a paleo BGHSZ, or a paleo free gas zone (Netzeband *et al.*, 2010; Bünz *et al.*, 2012). However, as we have already mentioned in the interpretation section, the stratigraphically-bound nature of the pipes and their root zones, with a root zone visually incompatible with any BGHSZ at the time of pipe formation, allows us to rule out gas hydrates dissociation as triggering mechanism for pipe formation.

The flat nature of the stratigraphic succession at the root zones and the widespread extension of the observed pipes would rule out any overpressure generated by the buoyancy of a hydrocarbon column in a conventional structural trap, especially considering the fact that a fracturing event caused by the buoyancy of a hydrocarbon column would be focused over a crestal point of a trap (Cartwright *et al.*, 2007), instead of over such a widespread area (~2500 km²).

The generation, exsolution/ebullition, or expansion of hydrocarbon fluids could be a viable mechanism for the generation of high overpressures and has been inferred by many observational and modelling results (Luo and Vasseur, 1996; Osborne and Swarbrick, 1997; Katahara and Corrigan, 2001; Scandella *et al.*, 2011; Bertoni *et al.*, 2013; Riboulot *et al.*, 2013; Tingay *et al.*, 2013). The generation and/or accumulation of hydrocarbon at the root zones of the pipe could thus be capable of triggering their formation. According to Osborne and Swarbrick (1997), the overpressure potential increases in parallel with the kinetics of the hydrocarbon generation process (i.e. a fast generation results in greater overpressure), as well as with the quality of the potential source rock generating hydrocarbon.

The two principal source rocks for thermogenic hydrocarbons in the GSCB are represented by mid to late Cretaceous marine and coastal coaly sediments, and by deep marine Early Paleocene organic-rich shales (i.e. the Tartan/Waipawa Formation) (Schjølter *et al.*, 2010; Hollis *et al.*, 2014; Sahoo *et al.*, 2014; Sahoo *et al.*, 2015). The publicly available information about hydrocarbon generation in the GSCB all point out towards a generation window between the late Paleocene and the early-mid Eocene for Mid-Late Cretaceous source rocks within the deepest parts of the basin (Kroeger and Funnell, 2012; Sahoo *et al.*, 2015). In the proximity of the identified pipes HC generation commenced at the end of the Cretaceous, but has been ongoing until present day. Depending on the position within the syn-rift half grabens (central versus flanks), Cretaceous source rocks expelled hydrocarbons at different times. According to

recent basin modelling the Paleocene source rocks are immature within the AOI of this study (OMV internal report).

The results from the wells most recently drilled in the contiguous deep-water Canterbury basin show also the potential for a late Cretaceous marine source rock, associated to a maximum flooding surface following the full marine transgression (Blanke, 2015). Although the potential Cretaceous source rock interval matches that of the root zone of the pipes, their burial depths at the time of pipe formation (150-595m), combined with the expected geothermal gradient at that time (i.e. during early post-rift conditions, ca. 35-43°C/km, cf. Sahoo and Bland, 2017; we used modified values based on internal regional OMV reports which indicate 38-56°C/km), would not be consistent with the generation of thermogenic hydrocarbons which, conversely, are predicted to be actively generating only at this stratigraphic interval, with onset of expulsion in the Early Eocene only in the deepest portions of the Great South Basin (Sahoo and Bland, 2017). Furthermore a triggering effect due to thermogenic hydrocarbons would result in pipes either above the mature kitchens (vertical migration) or above the highs (leakage through unconsolidated top seals) within the basin. However, the pipes within the area of interest are equally distributed over the highs as well as over the potential hydrocarbon kitchens and show no correlation with the structural configuration of the basin.

Based on the above observations, we consider the following scenario as the most likely explanation for the pipe occurrences. The root zone of the pipes, at the time of their generation, was likely situated at horizons K90-K80 therefore within a range of burial depths and temperature which could have led to the generation of biogenic gas (Figure 12) Basin modelling performed by OMV (OMV Internal Report) confirms this scenario (Figure 12). The extent of the pipe province mapped on the 3D dataset is spatially coincident with the modelled area of biogenic gas productivity, pointing to a causal link between pipes formation and biogenic gas generation in the Paleocene. The root zone of the pipes at the time of their generation coincides with an organic rich Late Cretaceous shale, encountered by Caravel-1. Based upon basin modelling results biogenic gas production occurred shortly before and during the generation of the pipes. Sudden pore pressure increase at the root zone of pipe-like conduits because of lateral and vertical pressure transfer requires a system of hydraulically-linked pressure compartments (Grauls and Baleix, 1994; Finkbeiner *et al.*, 2001; Flemings *et al.*, 2002; Tingay *et al.*, 2007; Leduc *et al.*, 2013; Tingay *et al.*, 2013). Although the link between widespread overpressures related to biogenic gas generation are not completely understood, recent studies show that early overpressure can occur in organic shales, and significant volumes of biogenic gas generation can lead to overpressure build-up (see e.g. Meng *et al.* 2017).

In addition to the above, Schiøler et al. (2010) and Hollis et al. (2014) suggested, based on palynological, geochemical, and sedimentological evidence that the occurrence of a eustatic sea-level fall in the late Paleocene, potentially associated with the formation of small ice sheets in the southern polar regions. Coincident with a drop in sea-level, the fine-grained low permeability Paleocene succession would have further facilitated the onset of water overpressure, due to the poroelastic effects on pore pressure in the presence of partially gas-saturated sediments (i.e. caused by gas expansion under undrained conditions, see Liu and Flemings, 2009).

Based on our stratigraphic interpretation of the termini of the fluid-escape pipes in the study area, we favour triggering events consisting of a combination of overpressure generated by volume expansion owing to biogenic gas generation. Eustatic fluctuations (i.e. sea-level falls) in the late Paleocene could then have contributed in the generation of critical overpressures at the root zones. Overall, the total amount of overpressure caused by hydrocarbon generation, exsolution and expansion could easily exceed the $\sim 1\text{--}6$ MPa required for fracturing the overburden between the root zones and the termini of the pipes (Osborne and Swarbrick, 1997; Swarbrick et al., 2001).

Global significance

The PETM was a global significant warming event that are regarded as close analogue to today's climate change. (Bowen et al. 2015). The proposed cause of PETM include a widespread gas hydrate dissociation, volcanic and intrusive-related processes, wetland methane emission, as well as desiccation of epicontinental seas and oxidation of organic carbon (Katz et al., 1999; Thomas et al., 2002; Svensen et al., 2004; Higgins and Schrag, 2006; Storey et al., 2007; Dickens, 2011; Aarnes et al., 2015). The studied system of pipes predate the PETM. However, we do not exclude that the emission of hydrocarbon at the seafloor from fluid-escape pipes can be a contributory element to climate global warming at the Paleocene-Eocene boundary, particularly considering the vast size of the pipe field identified in this study (see Judd, 2003; McGinnis et al., 2006; Römer et al., 2017). We suggest that hydrocarbon influx into the atmosphere from hydrocarbon plumbing systems characterised by vertical cross-stratal fluid-flow towards shallow water depths could represent an additional sources of greenhouse gases into the atmosphere to take into account for the later PETM. A thorough well calibration, pre-stack analysis of seismic data in the presence of reliable DHIs, and further data inputs into the basin modelling (rate of methane generation, source rock area and migrated methane from source rock) would be needed in order to provide an accurate estimate of the amount of gas produced by the documented expulsion events.

Late Jurassic and Cretaceous organic-rich fine-grained sediments have global significance as representing indicators of oceanic anoxic events and being important source rocks, leading to the formation of more than two thirds of the known hydrocarbon conventional resources (Jenkyns, 2010; Sorkhabi, 2016). Depending on the burial and thermal history of basins hosting such source rocks, the late Paleocene could have represented a critical period for hydrocarbon generation and expulsion and, in the absence of effective traps, could have resulted in significant leakage of these fluids, potentially enhanced by sea-level and temperature fluctuations.

The nature of the hydrocarbon fluids expelled along the fluid-escape pipes described here remain uncertain, but were most likely generated by microbial processes and therefore mainly comprised methane.

Overall, the observation and the interpretation of fossil systems of fluid-escape features in sedimentary basins provide invaluable information on the history of a basin, in terms of overpressure generation and fluid expulsion history. Moreover, these paleo-conduits, if not pervasively cemented by authigenic minerals, can remain permeable pathways for hydrocarbon and pore waters over time, therefore facilitating the migration of fluid at shallower depths even millions of years after their formation. Integrating these vertical fluid drainage systems into standard basin models, where fluid flow is primarily assumed to be controlled by stratal rather than cross-stratal pathways, would help in refining the prediction of overpressure, as well as economically prospective zones in a basin.

CONCLUSIONS

We have identified one of the largest deeply buried fluid escape pipe provinces observed worldwide, hosted in Cretaceous - late Paleocene sediments of the Great South and Canterbury Basin (NZ). This large buried pipe province totals a number of >2000 pipes over an area of ca. 2500 km², with maximum density of > 3 pipes/km².

The pipes are identified on 3D seismic data as subtle columnar disturbance zones, originated during discrete episodes of fluid venting, which disrupted the typical progressive basinal compaction-driven pore fluid expulsion. Their upper termini are defined by small-scale dome-shaped structures, indicating an associated constructional edifice. The majority of pipes terminate at late Paleocene horizons. The upper termini appear as small-scale dome-shaped structures on mapped 3D seismic surfaces, indicating edifice construction on contemporaneous seabed. These upper termini concentrate on late Paleocene horizons, thus constraining the time of pipe formation.

The majority of the lower termini are associated with a transgressive shale event in Late Cretaceous, suggesting a fluid source within the early post-rift sequence. Basin modelling indicates that the nature of the fluid is biogenic gas generated from near the root zone. Spatial alignment analysis of upper pipe termini reveals that pipe distribution is not affected by structural or sedimentological features while they spread over a wide area over both structural highs and depocentres.

Stratigraphic interpretation of fluid-escape pipe termini favour a triggering mechanism combined from volume expansion-generated overpressure owing to biogenic hydrocarbon production, and late Palaeocene eustatic sea level fall. A much smaller pipe group is observed in the early-mid Eocene that are more likely to be related to later HC generation and migration phase.

This study provides an example of how observation and the interpretation of a fossil systems of fluid-escape features in sedimentary basins conveys important information on the history of sedimentary basins, in particular on overpressure generation. These pipes paleo-conduits, if not pervasively cemented by authigenic minerals, can remain permeable pathways for hydrocarbon and pore waters over time, therefore facilitating the migration of fluid at shallower depths even millions of years after their formation.

ACKNOWLEDGEMENTS

This study was made possible thanks to the data initially provided by Shell and subsequently integrated by OMV. We gratefully acknowledge their contribution, and permission from OMV and JV partner Mitsui E&P Australia to publish the most recent basin modelling results. Schlumberger is thanked for the use of the Petrel software. Two anonymous reviewers and the editor are gratefully acknowledged for their comments which significantly helped improve the initial manuscript. Martino Foschi (<https://www.seismar.net>) has performed alignment analysis and produced the rose diagram. We also thank NZPAM for the release of 2D seismic lines and well data.

REFERENCES

- Aarnes, I., Planke, S., Trulsvik, M., Svensen, H., 2015. Contact metamorphism and thermogenic gas generation in the Vøring and Møre basins, offshore Norway, during the Paleocene–Eocene thermal maximum. *Journal of the Geological Society*, 172, 588-598.
- Andreassen, K., Hubbard, A., Winsborrow, M., Patton, H., Vadakkepuliambatta, S., Plaza-Faverola, A., Gudlaugsson, E., Serov, P., Deryabin, A., Mattingdal, R. and Mienert, J., 2017. Massive blow-out craters formed by hydrate-controlled methane expulsion from the Arctic seafloor. *Science*, 356, 948-953.
- Andresen, K.J., Huuse, M., Clausen, O.R., 2008. Morphology and distribution of Oligocene and Miocene pockmarks in the Danish North Sea—implications for bottom current activity and fluid migration. *Basin Res.*, 20, 445-466.
- Andresen, K.J., Huuse, M. 2011. ‘Bulls-eye’ pockmarks and polygonal faulting in the Lower Congo Basin: relative timing and implications for fluid expulsion during shallow burial. *Mar. Geol.*, 279, 111-127.
- Bache, F., Mortimer, N., Sutherland, R., Collot, J., Rouillard, P., Stagpoole, V., Nicol, A., 2014.. Seismic stratigraphic record of transition from Mesozoic subduction to continental breakup in the Zealandia sector of eastern Gondwana. *Gondwana Research*, 26, 1060-1078.
- Bertoni, C., Cartwright, J., Hermanrud, C., 2013. Evidence for large-scale methane venting due to rapid drawdown of sea level during the Messinian Salinity Crisis. *Geology*, 41, 371-374.
- Bertoni, C., Cartwright, J., Foschi, M. and Martin, J., 2018. Spectrum of gas migration phenomena across multi-layered sealing sequences. *AAPG Bull.*, V. 102, 1011-1034.
- Blanke, S.J. 2015 Caravel-1: Lessons Learned in the Deepwater Canterbury Basin. International Conference and Exhibition, Melbourne, Australia 13-16 September 2015.
- Bouriak, S., Vanneste, M., Saoutkine, A., 2000. Inferred gas hydrates and clay diapirs near the Storegga Slide on the southern edge of the Vøring Plateau, offshore Norway. *Mar. Geol.*, 163, 125-148.
- Bowen, G.J., Maibauer, B.J., Kraus, M.J., Röhl, U., Westerhold, T., Steimke, A., Gingerich, P.D., Wing, S.L., Clyde, W.C., 2015. Two massive, rapid releases of carbon during the onset of the Palaeocene– Eocene thermal maximum. *Nature Geoscience*, 8(1), p.44.
- Bünz, S., Polyanov, S., Vadakkepuliambatta, S., Consolaro, C., Mienert, J., 2012. Active gas venting through hydrate-bearing sediments on the Vestnesa Ridge, offshore W-Svalbard. *Mar. Geol.*, 332, 189-197.
- Cartwright, J., Huuse, M., Aplin, A., 2007. Seal bypass systems. *AAPG Bull.*, 91, 1141-1166.

- Cartwright, J.A., Santamarina, C. 2015. Seismic characteristics of fluid escape pipes in sedimentary basins: implications for pipe genesis. *Mar. Petrol. Geol.*, 65, 126-140.
- Chenrai, P., Huuse, M., 2017. Pockmark formation by porewater expulsion during rapid progradation in the offshore Taranaki Basin, New Zealand. *Mar. Petrol. Geol.*, 82, 399-413.
- Chopra, S., Marfurt, K.J., 2007. Seismic attributes for prospect identification and reservoir characterization. Society of Exploration Geophysicists and European Association of Geoscientists and Engineers.
- Chopra S., J. Castagna and O. Portniaguine, 2006, Seismic resolution and thin-bed reflectivity inversion: CSEG Recorder, 31, No. 01, 19-25.
- Cole, D., Stewart, S.A., Cartwright, J.A., 2000. Giant irregular pockmark craters in the Palaeogene of the outer Moray Firth basin, UK North Sea. *Mar. Petrol. Geol.*, 17, 563-577.
- Constable, R.M., Langdale, S., Allan, T.M.H., 2013. Development of a sequence stratigraphic framework in the Great South basin. Advantage NZ: 2013 Petroleum Conference. Wellington: NZPAM.
- Cook, R.A., Sutherland, R., Zhu, H., 1999. Cretaceous-Cenozoic geology and petroleum systems of the Great South Basin, New Zealand, Institute of Geological & Nuclear Sciences.
- Crutchley, G.J., Klaeschen, D., Planert, L., Bialas, J., Berndt, C., Papenberg, C., Hensen, C., Hornbach, M.J., Krastel, S., Brückmann, W., 2014. The impact of fluid advection on gas hydrate stability: Investigations at sites of methane seepage offshore Costa Rica. *Earth Planet. Sci. Lett.*, 401, 95-109.
- Davy, B., Pecher, I., Wood, R., Carter, L., Gohl, K., 2010. Gas escape features off New Zealand: Evidence of massive release of methane from hydrates. *Geophys. Res. Lett.*, 37, L21309.
- Dickens, G.R. 2011. Down the rabbit hole: Toward appropriate discussion of methane release from gas hydrate systems during the Paleocene-Eocene thermal maximum and other past events. *Climate of the Past*, 7, 831-846.
- Engelder, T., Fischer, M.P. 1994. Influence of poroelastic behavior on the magnitude of minimum horizontal stress, S_h in overpressured parts of sedimentary basins. *Geology*, 22, 949-952.
- Finkbeiner, T., Zoback, M., Flemings, P., Stump, B., 2001. Stress, pore pressure, and dynamically constrained hydrocarbon columns in the South Eugene Island 330 field, northern Gulf of Mexico. *AAPG Bull.*, 85, 1007-1031.
- Flemings, P.B., Stump, B.B., Finkbeiner, T., Zoback, M., 2002. Flow focusing in overpressured sandstones: Theory, observations, and applications. *Am. J. Sci.*, 302, 827-855.
- Flemings, P.B., Liu, X., Winters, W.J., 2003. Critical pressure and multiphase flow in Blake Ridge gas hydrates. *Geology*, 31, 1057-1060.
- Gay, A., Lopez, M., Cochonat, P., Séranne, M., Levaché, D., Sermondadaz, G., 2006. Isolated seafloor pockmarks linked to BSRs, fluid chimneys, polygonal faults and stacked Oligocene-Miocene turbiditic palaeochannels in the Lower Congo Basin. *Mar. Geol.*, 226, 25-40.

- Gay, A., Lopez, M., Berndt, C., Seranne, M., 2007. Geological controls on focused fluid flow associated with seafloor seeps in the Lower Congo Basin. *Mar. Geol.*, 244, 68-92.
- Gay, A., Mourgues, R., Berndt, C., Bureau, D., Planke, S., Laurent, D., Gautier, S., Lauer, C., Loggia, D., 2012. Anatomy of a fluid pipe in the Norway Basin: Initiation, propagation and 3D shape. *Mar. Geol.*, 332, 75-88.
- Giles, M.R., Indrelid, S.L., James, D.M.D., 1998. Compaction—the great unknown in basin modelling. *Geol. Soc. London, Spec. Publ.*, 141, 15-43.
- Grauls, D.J., Baleix, J.M. 1994. Role of overpressures and in situ stresses in fault-controlled hydrocarbon migration: A case study. *Mar. Petrol. Geol.*, 11, 734-742.
- Hansen, J.P.V., Cartwright, J.A., Huuse, M., Clausen, O.R., 2005. 3D seismic expression of fluid migration and mud remobilization on the Gjallar Ridge, offshore mid - Norway. *Basin Res.*, 17, 123-139.
- Hartwig, A., Anka, Z., di Primio, R., 2012. Evidence of a widespread paleo-pockmarked field in the Orange Basin: an indication of an early Eocene massive fluid escape event offshore South Africa. *Mar. Geol.*, 332, 222-234.
- Higgins, J.A., Schrag, D.P. 2006. Beyond methane: towards a theory for the Paleocene–Eocene thermal maximum. *Earth Planet. Sci. Lett.*, 245, 523-537.
- Hillman, J.I., Gorman, A.R., Pecher, I.A., 2015. Geostatistical analysis of seafloor depressions on the southeast margin of New Zealand's South Island—Investigating the impact of dynamic near seafloor processes on geomorphology. *Mar. Geol.*, 360, 70-83.
- Ho, S., Cartwright, J.A., Imbert, P., 2012. Vertical evolution of fluid venting structures in relation to gas flux, in the Neogene- Quaternary of the Lower Congo Basin, Offshore Angola. *Mar. Geol.*, 332, 40-55.
- Hollis, C.J., Dickens, G.R., Field, B.D., Jones, C.M., Strong, C.P., 2005. The Paleocene–Eocene transition at Mead Stream, New Zealand: a southern Pacific record of early Cenozoic global change. *Palaeogeogr., Palaeoclimatol., Palaeoecol.*, 215, 313-343.
- Hollis, C.J., Tayler, M.J., Andrew, B., Taylor, K.W., Lurcock, P., Bijl, P.K., Kulhanek, D.K., Crouch, E.M., Nelson, C.S., Pancost, R.D., Huber, M., 2014. Organic-rich sedimentation in the South Pacific Ocean associated with Late Paleocene climatic cooling. *Earth-Sci. Rev.*, 134, 81-97.
- Holtzman, R., Juanes, R. 2011. Thermodynamic and hydrodynamic constraints on overpressure caused by hydrate dissociation: A pore - scale model. *Geophys. Res. Lett.*, 38, L14308.
- Hunt International 1977. Final report Kawau-1A by Hunt International Petroleum Co NZ. PR716, Petroleum Report Series, MBIE New Zealand.
- Hustoft, S., Mienert, J., Bünz, S., Nouzé, H., 2007. High-resolution 3D-seismic data indicate focussed fluid migration pathways above polygonal fault systems of the mid-Norwegian margin. *Mar. Geol.*, 245, 89-106.

- Hustoft, S., Bünz, S., Mienert, J., 2010. Three - dimensional seismic analysis of the morphology and spatial distribution of chimneys beneath the Nyegga pockmark field, offshore mid - Norway. *Basin Res.*, 22, 465- 480.
- Iyer, K., Schmid, D.W., Planke, S. and Millett, J., 2017. Modelling hydrothermal venting in volcanic sedimentary basins: Impact on hydrocarbon maturation and paleoclimate. *Earth and Planetary Science Letters*, 467, pp.30-42.
- Jain, A.K., Juanes, R. 2009. Preferential mode of gas invasion in sediments: Grain - scale mechanistic model of coupled multiphase fluid flow and sediment mechanics. *J. Geophys. Res.: Solid Earth*, 114, B08101.
- Jenkyns, H.C. 2010. Geochemistry of oceanic anoxic events. *Geochem. Geophys. Geosyst.*, 11.
- Judd, A.G. 2003. The global importance and context of methane escape from the seabed. *Geo-Mar. Lett.*, 23, 147-154.
- Judd, A.G., Hovland, M. 2007. *Seabed Fluid Flow: The Impact on Geology, Biology and the Marine Environment*, Cambridge University Press.
- Kang, N.K., Yoo, D.G., Yi, B.Y., Park, S.C., 2016. Distribution and origin of seismic chimneys associated with gas hydrate using 2D multi-channel seismic reflection and well log data in the Ulleung Basin, East Sea. *Quatern. Int.*, 392, 99-111
- Katahara, K.W., Corrigan, J.D. 2001. Effect of Gas on Poroelastic Response to Burial or Erosion. In: Huffman, A.R. & Bowers, G.L. (eds.) *Pressure Regimes in Sedimentary Basins and Their Prediction*. AAPG Memoir, 76, 73-78.
- Katz, M.E., Pak, D.K., Dickens, G.R., Miller, K.G., 1999. The source and fate of massive carbon input during the latest Paleocene thermal maximum. *Science*, 286, 1531-1533.
- Killops, S.D., Hollis, C.J., Morgans, H.E.G., Sutherland, R., Field, B.D., Leckie, D.A., 2000. Paleooceanographic significance of Late Paleocene dysaerobia at the shelf/slope break around New Zealand. *Palaeogeogr., Palaeoclimatol., Palaeoecol.*, 156, 51-70.
- Kim, J.H., Torres, M.E., Choi, J., Bahk, J.J., Park, M.H., Hong, W.L., 2012. Inferences on gas transport based on molecular and isotopic signatures of gases at acoustic chimneys and background sites in the Ulleung Basin. *Org. Geochem.*, 43, 26-38.
- Kirkham, C., Cartwright, J., Hermanrud, C., Jebson, C., 2018. The genesis of mud volcano conduits through thick evaporite sequences. *Basin Res.*, 30, 217-236.
- Krämer, K., Holler, P., Herbst, G., Bratek, A., Ahmerkamp, S., Neumann, A., ... & Winter, C. (2017). Abrupt emergence of a large pockmark field in the German Bight, southeastern North Sea. *Scientific reports*, 7(1), 5150.)
- Kroeger, K.F., Funnell, R.H. 2012. Warm Eocene climate enhanced petroleum generation from Cretaceous source rocks: A potential climate feedback mechanism? *Geophys. Res. Lett.*, 39.

- Lavoie, D., Pinet, N., Duchesne, M., Bolduc, A., Larocque, R., 2010. Methane-derived authigenic carbonates from active hydrocarbon seeps of the St. Lawrence Estuary, Canada. *Mar. Petrol. Geol.*, 27, 1262-1272.
- Leduc, A.M., Davies, R.J., Swarbrick, R.E., Imber, J., 2013. Fluid flow pipes triggered by lateral pressure transfer in the deepwater western Niger Delta. *Mar. Petrol. Geol.*, 43, 423-433.
- Liu, X., Flemings, P.B. 2009. Dynamic response of oceanic hydrates to sea level drop. *Geophys. Res. Lett.*, 36, L17308.
- Løseth, H., Gading, M., Wensaas, L., 2009. Hydrocarbon leakage interpreted on seismic data. *Mar. Petrol. Geol.*, 26, 1304- 1319. Løseth, H., et al. 2011. 1000 m long gas blow-out pipes. *Mar. Petrol. Geol.*, 28, 1047-1060.
- Luo, X., Vasseur, G. 1996. Geopressuring mechanism of organic matter cracking: numerical modeling. *AAPG Bull.*, 80, 856-873.
- MacDonald, I.R., Bohrmann, G., Escobar, E., Abegg, F., Blanchon, P., Blinova, V., Brückmann, W., Drews, M., Eisenhauer, A., Han, X., Heeschen, K., 2004. Asphalt volcanism and chemosynthetic life in the Campeche Knolls, Gulf of Mexico. *Science*, 304, 999-1002.
- Maestrelli, D., Iacopini, D., Jihad, A.A., Bond, C.E., Bonini, M., 2017. Seismic and structural characterization of fluid escape pipes using 3D and partial stack seismic from the Loyal Field (Scotland, UK): A multiphase and repeated intrusive mechanism. *Mar. Petrol. Geol.*, 88, 489-510.
- Maia, A.R., Cartwright, J., Andersen, E., 2016. Shallow plumbing systems inferred from spatial analysis of pockmark arrays. *Mar. Petrol. Geol.*, 77, 865-881.
- Manton, B. 2015. The mechanics of sill propagation and associated venting, investigated using 3D seismic data from offshore Norway. Cardiff University.
- Matsumoto, R., Tanahashi, M., Kakuwa, Y., Snyder, G., Ohkawa, S., Tomaru, H., Morita, S., 2017. Recovery of thick deposits of massive gas hydrates from gas chimney structures, eastern margin of Japan Sea: Japan Sea Shallow Gas Hydrate Project. *Fire in the Ice*, 17, 1-6.
- McGinnis, D.F., Greinert, J., Artemov, Y., Beaubien, S.E., Wüest, A.N.D.A., 2006. Fate of rising methane bubbles in stratified waters: How much methane reaches the atmosphere? *J. Geophys. Res.: Oceans*, 111.
- Mcinerney, F.A., Wing, S.L. 2011. The Paleocene-Eocene Thermal Maximum: a perturbation of carbon cycle, climate, and biosphere with implications for the future. *Annual Review of Earth and Planetary Sciences*, 39, 489-516.
- Meadows, D., Davies, R.J. 2008. Predicting porosity reduction due to silica diagenesis using seismic reflection data. *Mar. Petrol. Geol.*, 26, 1-12.
- Meng, Q., Hooker, J., Cartwright, J., 2017. Early overpressuring in organic-rich shales during burial: evidence from fibrous calcite veins in the Lower Jurassic Shales-with-Beef Member in the Wessex Basin, UK. *Journal of the Geological Society*, 174(5), pp.869-882.

- Morley, C.K., Maczak, A., Rungprom, T., Ghosh, J., Cartwright, J.A., Bertoni, C., Panpichityota, N., 2017. New style of honeycomb structures revealed on 3D seismic data indicate widespread diagenesis offshore Great South Basin, New Zealand. *Marine and Petroleum Geology*, 86, pp.140-154.
- Moss, J.L., Cartwright, J.A. 2010. 3D seismic expression of km - scale fluid escape pipes from offshore Namibia. *Basin Res.*, 22, 481-501.
- Mourgues, R., Gressier, J.B., Bodet, L., Bureau, D., Gay, A., 2011. "Basin scale" versus "localized" pore pressure/stress coupling–Implications for trap integrity evaluation. *Mar. Petrol. Geol.*, 28, 1111-1121.
- Naudts, L., Greinert, J., Artemov, Y., Staelens, P., Poort, J., Van Rensbergen, P., De Batist, M., 2006. Geological and morphological setting of 2778 methane seeps in the Dnepr paleo-delta, northwestern Black Sea. *Mar. Geol.*, 227, 177-199.
- Nelson, P.H. 2009. Pore-throat sizes in sandstones, tight sandstones, and shales. *AAPG Bull.*, 93, 329- 340.
- Netzeband, G.L., Krabbenhöft, A., Zillmer, M., Petersen, C.J., Papenberg, C., Bialas, J., 2010. The structures beneath submarine methane seeps: seismic evidence from Opouawe Bank, Hikurangi Margin, New Zealand. *Mar. Geol.*, 272, 59-70.
- Nicolo, M.J., Dickens, G.R., Hollis, C.J., Zachos, J.C., 2007. Multiple early Eocene hyperthermals: Their sedimentary expression on the New Zealand continental margin and in the deep sea. *Geology*, 35, 699-702.
- O'Brien, G.W., Lawrence, G.M., Williams, A.K., Glenn, K., Barrett, A.G., Lech, M., Edwards, D.S., Cowley, R., Boreham, C.J., Summons, R.E., 2005. Yampi Shelf, Browse Basin, North-West Shelf, Australia: a test-bed for constraining hydrocarbon migration and seepage rates using combinations of 2D and 3D seismic data and multiple, independent remote sensing technologies. *Marine and Petroleum Geology*, 22(4), pp.517-549.
- Osborne, M.J., Swarbrick, R.E. 1997. Mechanisms for generating overpressure in sedimentary basins: a reevaluation. *AAPG Bull.*, 81, 1023-1041.
- Paganoni, M., Cartwright, J.A., Foschi, M., Shipp, C.R., Van Rensbergen, P., 2018. Relationship between fluid-escape pipes and hydrate distribution in offshore Sabah (NW Borneo). *Mar. Geol.*, 395, 82-103.
- Paull, C.K., Ussler, W., Dallimore, S.R., Blasco, S.M., Lorenson, T.D., Melling, H., Medioli, B.E., Nixon, F.M., McLaughlin, F.A., 2007. Origin of pingo - like features on the Beaufort Sea shelf and their possible relationship to decomposing methane gas hydrates. *Geophys. Res. Lett.*, 34.
- Paull, C.K., Normark, W.R., Ussler III, W., Caress, D.W., Keaten, R., 2008. Association among active seafloor deformation, mound formation, and gas hydrate growth and accumulation within the seafloor of the Santa Monica Basin, offshore California. *Mar. Geol.*, 250, 258-275.

- Pearson, A.R. 1998. The Great South Basin–Antrim International’s Exploration Strategy. Proceedings of the 1998 New Zealand Petroleum Conference. Ministry of Commerce, Wellington.
- Planke, S., Rasmussen, T., Rey, S.S., Myklebust, R., 2005. Seismic characteristics and distribution of volcanic intrusions and hydrothermal vent complexes in the Vøring and Møre basins. Geological Society, London, Petroleum Geology Conference series.
- Plaza-Faverola, A., Bünz, S., Mienert, J., 2011. Repeated fluid expulsion through sub-seabed chimneys offshore Norway in response to glacial cycles. *Earth Planet. Sci. Lett.*, 305, 297-308.
- Plaza-Faverola, A., Bünz, S., Johnson, J.E., Chand, S., Knies, J., Mienert, J., Franek, P., 2015. Role of tectonic stress in seepage evolution along the gas hydrate charged Vestnesa Ridge, Fram Strait. *Geophys. Res. Lett.*, 42, 733-742.
- Pryer, L., J. Weir, T. Debacker, and K. Romine, 2013, Interpretation of basement: NZ ECS SEEBASE: Advantage New Zealand Petroleum Summit, April 2013.
- Riboulot, V., Cattaneo, A., Sultan, N., Garziglia, S., Ker, S., Imbert, P., Voisset, M., 2013. Sea-level change and free gas occurrence influencing a submarine landslide and pockmark formation and distribution in deepwater Nigeria. *Earth Planet. Sci. Lett.*, 375, 78-91.
- Riboulot, V., Thomas, Y., Berné, S., Jouet, G., Cattaneo, A., 2014. Control of Quaternary sea - level changes on gas seeps. *Geophys. Res. Lett.*, 41, 4970-4977.
- Roberts, H.H., Hardage, B.A., Shedd, W.W., Hunt Jr, J., 2006. Seafloor reflectivity—an important seismic property for interpreting fluid/gas expulsion geology and the presence of gas hydrate. *The Leading Edge*, 25, 620-628.
- Römer, M., Wenau, S., Mau, S., Veloso, M., Greinert, J., Schlüter, M., Bohrmann, G., 2017. Assessing marine gas emission activity and contribution to the atmospheric methane inventory: A multidisciplinary approach from the Dutch Dogger Bank seep area (North Sea). *Geochem. Geophys. Geosyst.*
- Sager, W.W., MacDonald, I.R., Hou, R., 2003. Geophysical signatures of mud mounds at hydrocarbon seeps on the Louisiana continental slope, northern Gulf of Mexico. *Mar. Geol.*, 198, 97-132.
- Sahoo, T., King, P., Bland, K., Strogen, D., Sykes, R., Bache, F., 2014. Tectono-sedimentary evolution and source rock distribution of the mid to Late Cretaceous succession in the Great South Basin, New Zealand. *The APPEA Journal*, 54, 259- 274.
- Sahoo, T.R., Kroeger, K.F., Thrasher, G., Munday, S., Mingard, H., Cozens, N., Hill, M., 2015. Facies Distribution and Impact on Petroleum Migration in the Canterbury Basin, New Zealand. International Conference & Exhibition.
- Sahoo, T.R., Bland, K.J. 2017. Atlas of Petroleum Prospectivity, Southeast Province: ArcGIS geodatabase and technical report. GNS Science Data Series 23c, October 2017.
- Scandella, B.P., Varadharajan, C., Hemond, H.F., Ruppel, C., Juanes, R., 2011. A conduit dilation model of methane venting from lake sediments. *Geophys. Res. Lett.*, 38.

- Schiøler, P., Rogers, K., Sykes, R., Hollis, C.J., Ilg, B., Meadows, D., Roncaglia, L., Uruski, C., 2010. Palynofacies, organic geochemistry and depositional environment of the Tartan Formation (Late Paleocene), a potential source rock in the Great South Basin, New Zealand. *Mar. Petrol. Geol.*, 27, 351-369.
- Serié, C., Huuse, M., Schødt, N.H., 2012. Gas hydrate pingoes: Deep seafloor evidence of focused fluid flow on continental margins. *Geology*, 40, 207-210.
- Serié, C., Huuse, M., Schødt, N.H., Brooks, J.M. and Williams, A., 2017. Subsurface fluid flow in the deep - water Kwanza Basin, offshore Angola. *Basin Res.*, 1-31.
- Sloan Jr, E.D., Koh, C., 2007. Clathrate hydrates of natural gases. CRC press.
- Somoza, L., León, R., Medialdea, T., Pérez, L.F., González, F.J., Maldonado, A., 2014. Seafloor mounds, craters and depressions linked to seismic chimneys breaching fossilized diagenetic bottom simulating reflectors in the central and southern Scotia Sea, Antarctica. *Global Planet. Change*, 123, 359-373.
- Sorkhabi, R. 2016. Rich Petroleum Source Rocks. *GeoExPro*, 6. Stewart, S.A. & Davies, R.J. 2006. Structure and emplacement of mud volcano systems in the South Caspian Basin. *AAPG Bull.*, 90, 771-786.
- Stolper, D.A., Lawson, M., Davis, C.L., Ferreira, A.A., Neto, E.S., Ellis, G.S., Lewan, M.D., Martini, A.M., Tang, Y., Schoell, M., Sessions, A.L., 2014. Formation temperatures of thermogenic and biogenic methane. *Science*, 344, 1500-1503.
- Storey, M., Duncan, R.A., Swisher, C.C., 2007. Paleocene-Eocene thermal maximum and the opening of the northeast Atlantic. *Science*, 316, 587-589.
- Sultan, N., Cochonat, P., Foucher, J.P., Mienert, J., 2004. Effect of gas hydrates melting on seafloor slope instability. *Mar. Geol.*, 213, 379-401.
- Sultan, N., Riboulot, V., Ker, S., Marsset, B., Geli, L., Tary, J.B., Klingelhoefer, F., Voisset, M., Lanfumey, V., Colliat, J.L., Adamy, J., 2011. Dynamics of fault - fluid - hydrate system around a shale - cored anticline in deepwater Nigeria. *J. Geophys. Res.: Solid Earth*, 116, B12110.
- Sun, Q., Wu, S., Cartwright, J., Dong, D., 2012. Shallow gas and focused fluid flow systems in the Pearl River Mouth Basin, northern South China Sea. *Mar. Geol.*, 315, 1-14.
- Svensen, H., Planke, S., Malthe-Sørenssen, A., Jamtveit, B., Myklebust, R., Eidem, T.R., Rey, S.S., 2004. Release of methane from a volcanic basin as a mechanism for initial Eocene global warming. *Nature*, 429, 542-545.
- Swarbrick, R.E., Osborne, M.J., Yardley, G.S., 2001. *AAPG Memoir 76, Chapter 1: Comparison of Overpressure Magnitude Resulting from the Main Generating Mechanisms.*
- Talukder, A.R., Bialas, J., Klaeschen, D., Bürk, D., Brückmann, W., Reston, T., Breitzke, M., 2007. High-resolution, deep tow, multichannel seismic and sidescan sonar survey of the submarine mounds and associated BSR off Nicaragua pacific margin. *Mar. Geol.*, 241, 33-43.

- Thomas, D.J., Zachos, J.C., Bralower, T.J., Thomas, E., Bohaty, S., 2002. Warming the fuel for the fire: Evidence for the thermal dissociation of methane hydrate during the Paleocene-Eocene thermal maximum. *Geology*, 30, 1067-1070.
- Tingay, M.R., Morley, C.K., Laird, A., Limpornpipat, O., Krisadasima, K., Pabchanda, S., Macintyre, H.R., 2013. Evidence for overpressure generation by kerogen-to-gas maturation in the northern Malay Basin. *AAPG Bull.*, 97, 639-672.
- Tingay, M.R., Hillis, R.R., Swarbrick, R.E., Morley, C.K., Damit, A.R., 2007. 'Vertically transferred' overpressures in Brunei: Evidence for a new mechanism for the formation of high-magnitude overpressure. *Geology*, 35, 1023-1026.
- Uruski, C., Ilg, B. 2006. Preliminary Interpretation and Structural Modelling of DUN06 Seismic Reflection Data from Great South Basin, Offshore New Zealand. GNS Science Consultancy, 46.
- Uruski, C. 2015. The contribution of offshore seismic data to understanding the evolution of the New Zealand continent. *Geol. Soc. London, Spec. Publ.*, 413, 35-51.
- Valentine, D.L. 2011. Emerging topics in marine methane biogeochemistry. *Annu. Rev. Mar. Sci.*, 3, 147-171.
- Van Rensbergen, P., Rabaute, A., Colpaert, A., Ghislain, T.S., Mathijs, M., Bruggeman, A., 2007. Fluid migration and fluid seepage in the Connemara Field, Porcupine Basin interpreted from industrial 3D seismic and well data combined with high-resolution site survey data. *International Journal of Earth Sciences*, 96, 185-197.
- Waghorn, K.A., Pecher, I., Strachan, L.J., Crutchley, G., Bialas, J., Coffin, R., Davy, B., Koch, S., Kroeger, K.F., Papenberg, C. and Sarkar, S., 2018. Paleo - fluid expulsion and contouritic drift formation on the Chatham Rise, New Zealand. *Basin Research*, 30(1), pp.5-19.
- Wandres, A., Bradshaw, J. 2005. New Zealand tectonostratigraphy and implications from conglomeratic rocks for the configuration of the SW Pacific margin of Gondwana. *Geological Society, London, Special Publications*, 246, 179-216.
- Widess, M.B. 1973. How thin is a thin bed? *Geophysics*, 38, 1176-1180.
- Xu, W., Germanovich, L.N. 2006. Excess pore pressure resulting from methane hydrate dissociation in marine sediments: A theoretical approach. *J. Geophys. Res.: Solid Earth*, 111, B01104.
- Zachos, J.C., Dickens, G.R., Zeebe, R.E., 2008. An early Cenozoic perspective on greenhouse warming and carbon-cycle dynamics. *Nature*, 451, 279-283.

FIGURE CAPTIONS

Figure 1 a) Location map of study area, in the Great South and Canterbury Basin, offshore New Zealand South Island. The basin depocentres are highlighted by short-dashed lines, while the current shelf location is marked by a long-dashed line. The black box indicates the Tawhaki - Rigel 3D seismic survey; light blue lines indicate 2D seismic lines. The colour shaded areas indicate the different basement terranes according to Wandres and Bradshaw (2005) and Pryer et al. (2013). The Great South and Canterbury Basin are underlain by a pre-rift sequence of Late Paleozoic to Jurassic/Cretaceous age, composed by the Murihuku, Dun Mountain - Maitai and Caples South terranes. B) Regional 2D seismic composite section showing long-distance tie of the 3D seismic survey area (location in Figure 1b). The Tara-1 and Toroa-1 wells drilled an almost complete stratigraphic section, down to the Cretaceous sediments. The Tara-1 inverted anticline is related to the Southern Alps tectonic compressional phase. The Murihuku reflective basement terrane is present in the NE part of the section, while the other terranes imaged are nearly acoustically transparent. Map and section modified after Bertoni et al. (2018).

Figure 2 Schematic diagram showing basin history and stratigraphy (for both the Great South and Canterbury Basins, offshore New Zealand's South Island). The horizons used throughout the paper are also shown. PG: WF: LF: TF: HG: Hoiho Group (OMV Internal Report). Blue arrows indicate prevalence of extension (during the rifting phase, outwards arrows), of subsidence (downwards arrows) and of uplift (upwards arrows). Coloured circles indicate elements of the petroleum system; SR: source rock (green), S: seal (blue), R: reservoir (yellow).

Figure 3 Seismic section across the 3D seismic survey (location in Figure 1), showing the stratigraphic setting of the main horizons in the interval of interest. The syn-rift unit (top basement to K50) is arranged into asymmetric, half-graben wedges. The Hoiho Group source rocks in the study area are located at horizons K20, K50 in the syn-rift series, and K80 in the early post-rift series. The early post-rift interval (horizons K50 to T50) exhibits a wedged shape, thinning towards the ESE, which is the part of the study area where the fluid escape pipes are present. Horizon T10 is an important regional marker within the post-rift series, and it corresponds to the Tartan or Waipawa organic shales.

Figure 4 Seismic section across the 3D seismic survey (location in Figure 1) DR: diagenetic reflector (silica diagenesis), AA: amplitude anomalies. The K80-T10 unit, where it hosts the pipes, is seismically characterised by parallel reflections with a consistently high-amplitude character, and by the absence of large scale gas-related amplitude such as the ones described by Bertoni et al. (2018) in the SW and NW part of the 3D survey area. This laterally continuous layered sequence is locally disrupted by a set of columnar zones having a chaotic-to-transparent seismic character. These are interpreted as fluid escape pipes (see text for details).

Figure 5 a) TWT (Isochron) and b) Depth converted thickness map of the K80-T00 interval, with the extent of the area covered by the mapped columnar disturbance zones, interpreted as fluid escape pipes, marked by the grey transparency. The regionally mapped K80 interval is used as a proxy for the overlying K90 shale, which is not clearly mappable due to imaging issues. Location of line indicated in Figure 1.

Figure 6 a) Seismic section across the 3D seismic survey (location in Figure 2 and 6b). The upper termini of the main fluid escape pipes are highlighted with a black circle. The arrows point to the unequivocal root zones of the fluid escape pipes. This generally corresponds to the larger columnar features associated with breaks in reflection continuity. b) Variance extraction on horizon T00, showing the circular structures that correspond to the upper termini of the fluid escape pipes. They display a diameter of a few 100s of meters. The solid white line shows the location of seismic line in Figure 6a. c) Zoom of seismic section in Figure 6a, with details of upper termini and root zones of the pipes.

Figure 7 3D perspective view of the time-structure map of horizon T00 (location in Figure 5). The positive relief and mounded morphology mark the upper termini of the columnar disturbance zones. These are characterised by convex upwards morphology and display a positive relief of approximately 30-50 ms on horizon T00, similarly to what observed, in smaller numbers, on horizons T10 (late Paleocene), and occasionally, T50 (early-mid Eocene). Highlighted are only a few of the mounded structures (white arrows), as a guidance to the identification of similar structures that populate the entire surface.

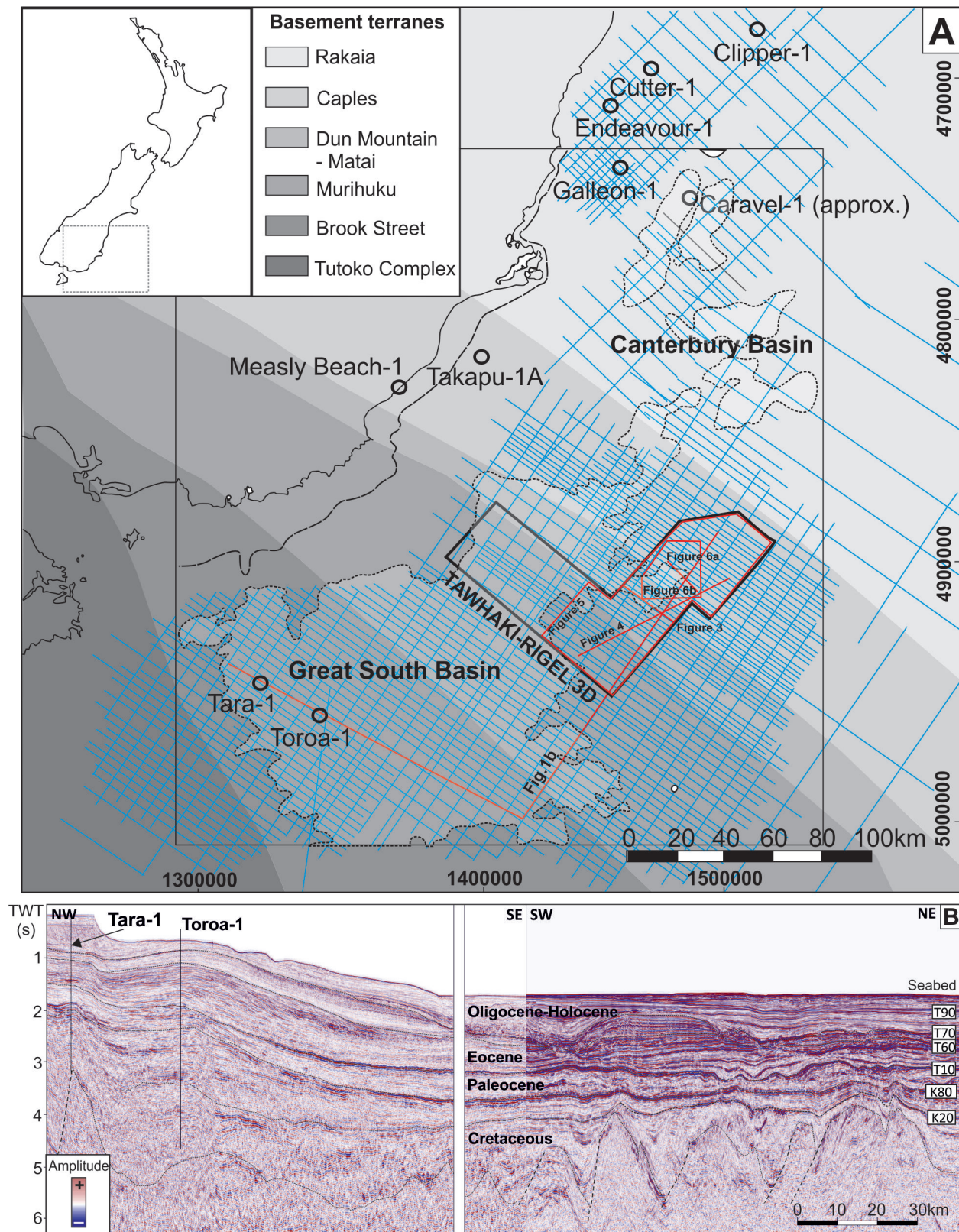
Figure 8 a) Variance extraction on horizon T00. The high-variance black dots are the upper termini of the fluid escape pipes, which reach maximum density/areal coverage on T00. b) TWT map of horizon T00 with location of fluid escape pipes (red dots), cumulatively with upper termini on T00, T10 and T50. c) Spatial alignment analysis of the pipes upper termini, considering the average nearest neighbour univariate spatial autocorrelation statistical method. The distribution is widely scattered, with no preferential alignment. d) Interpreted water depths/paleoenvironments at the time of T10 formation, also representative of T00. The distribution of the fluid escape pipes roughly coincides with the deeper, slope to basin floor depositional environments.

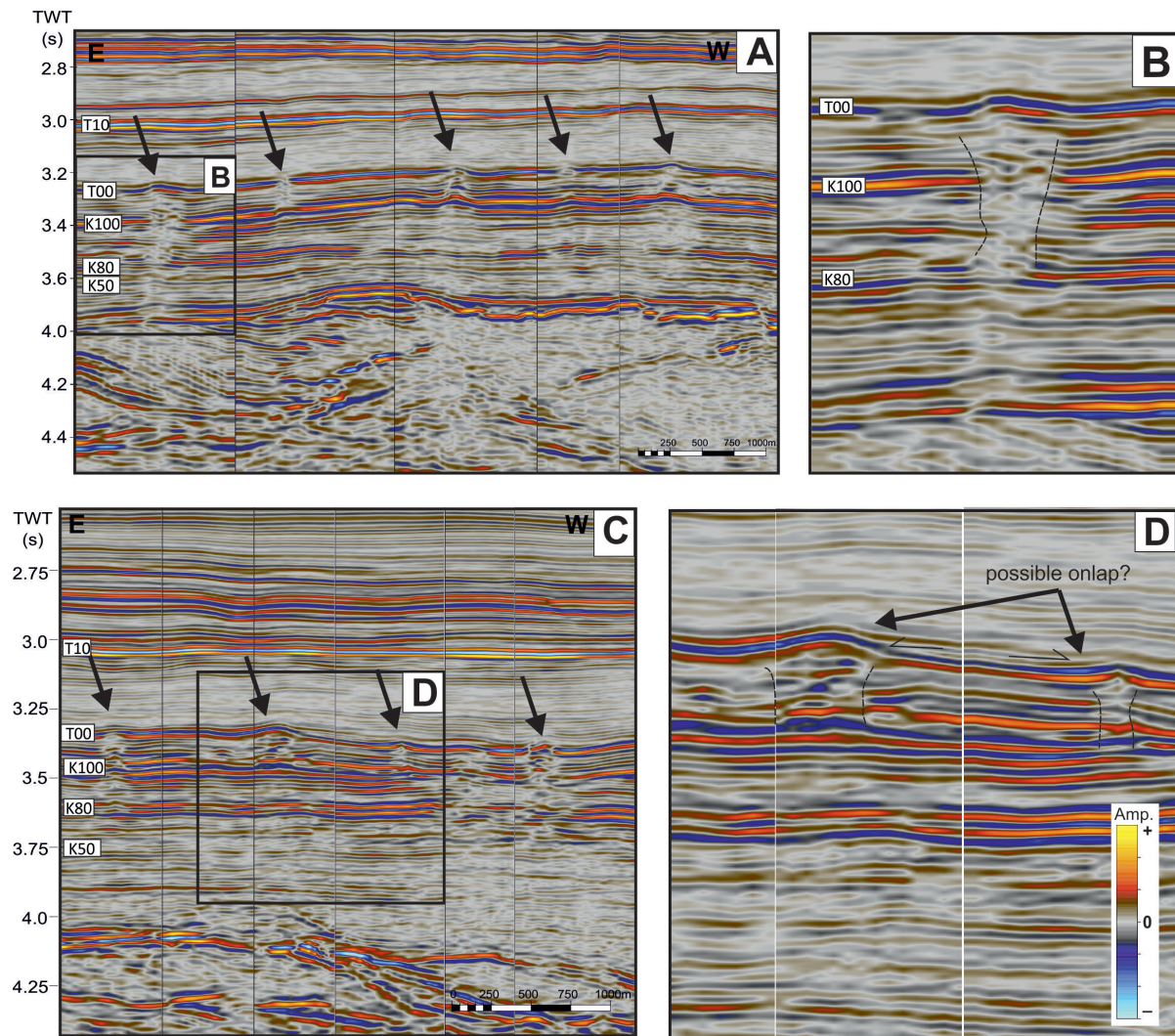
Figure 9 Seismic section across the 3D seismic survey (location in Figure 5). Black arrows mark the upper termini of the most evident pipes. While most of the pipes terminate upwards on horizon T00, and on horizon T10, there are sporadic examples of upper termini on horizon T50: three clear examples are evidenced on this seismic section with red arrows.

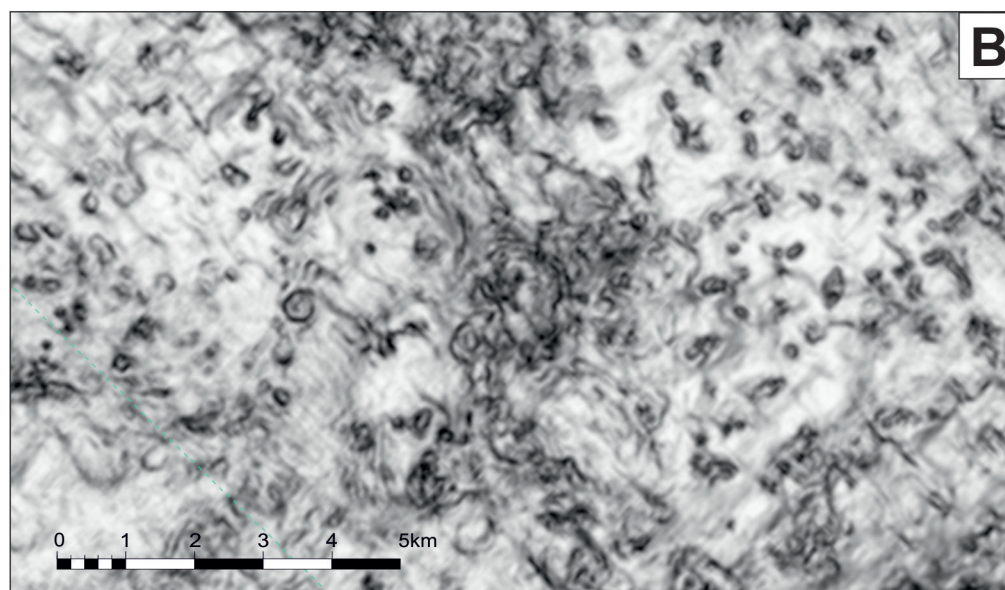
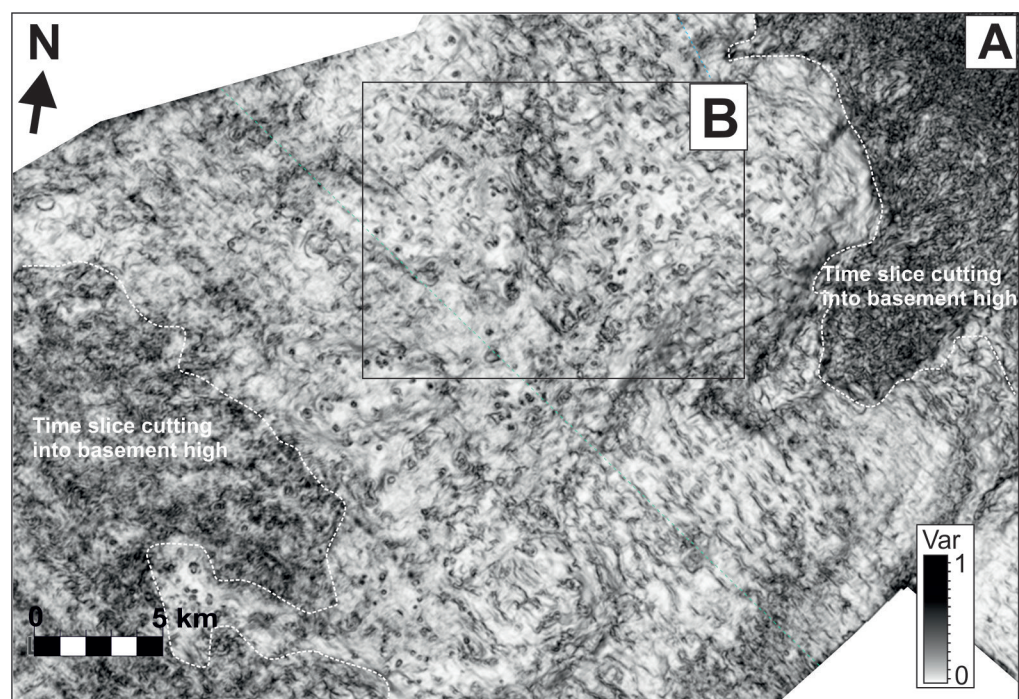
Figure 10 Seismic sections across the 3D seismic survey (location in Figure 5). Figures a) and c), and their zoomed details in b) and d), show: the pipes upper termini (indicated by black arrows), conduit interpretation (dotted black lines), associated attenuation of seismic amplitudes, onlap of pipes overburden on top of horizon T00.

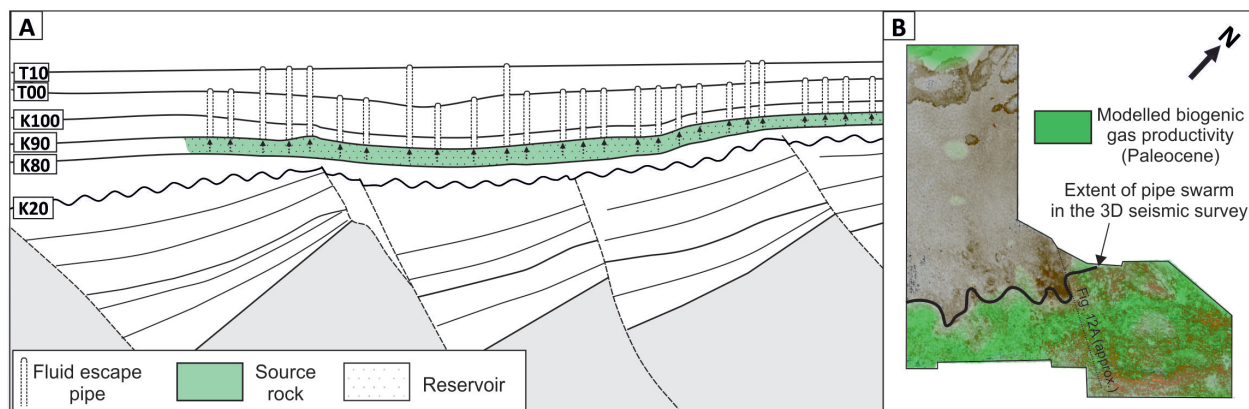
Figure 11 a) Time slice of the variance volume of the 3D survey (3444ms), and b) zoom, showing the horizontal section of the pipes conduits (Location in Figure 8). The horizontal sections of the pipes show subcircular to elliptical and irregular morphology, which enclose areas of high variance anomalies (high values of reflection lateral discontinuities). The morphology of the pipes section could be distorted to the time-concordant nature of the time-slice and therefore oblique to horizon-based extractions (see e.g. Fig. 6B and 8A). However, this time slice display is still valuable because it shows with great clarity the neat margins of the pipe conduits and their size. The white dashed lines mark the boundary of the extension of the pipe field, and loss of imaging of the pipe conduits, due to the intersection of the time slice with deeper structural highs.

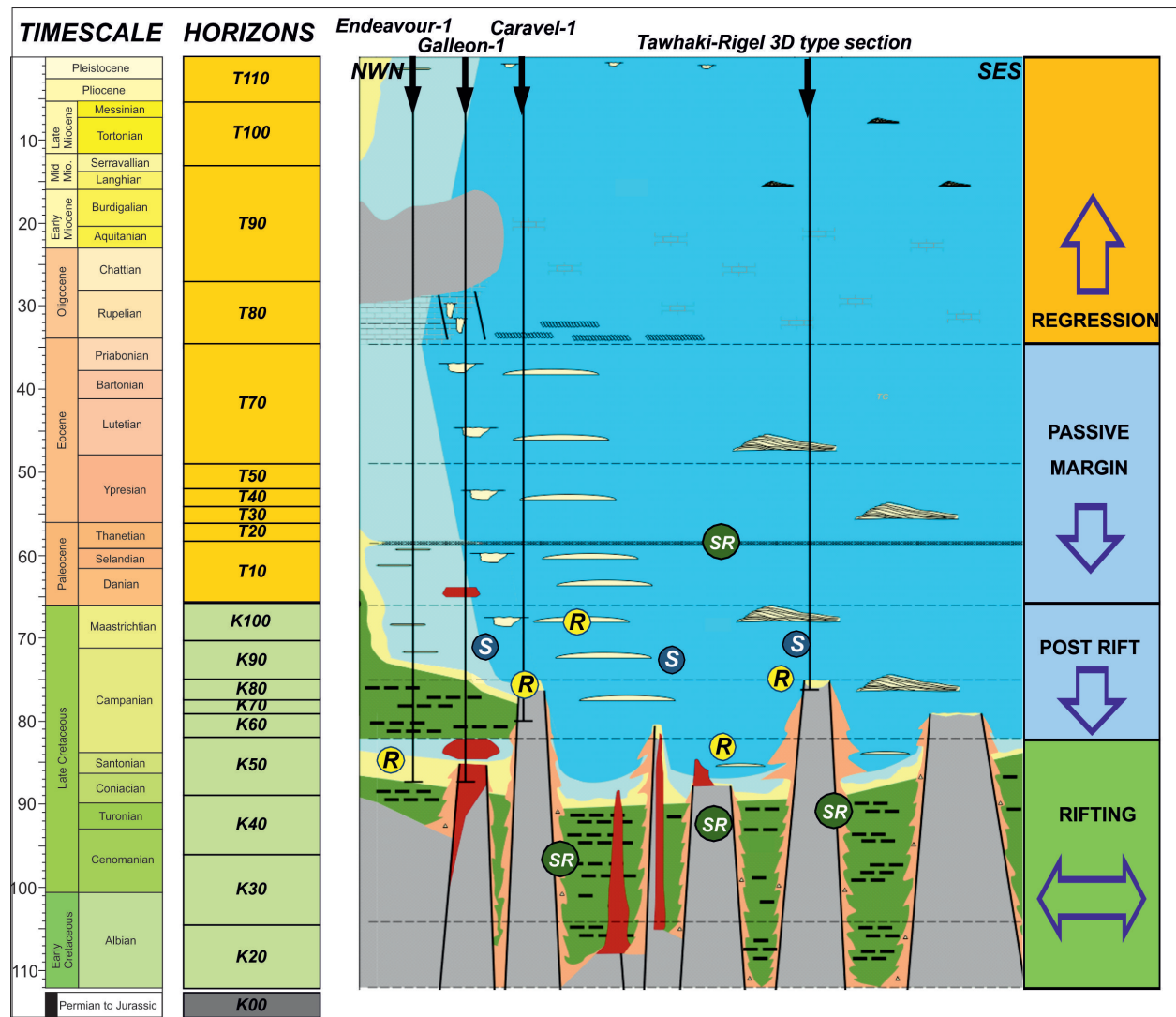
Figure 12 a) Schematic diagram illustrating the model of pipe formation by generation and expulsion of biogenic gas. The potential source rock is located at horizon K90 (just above horizon K80, used as a mapping reference due to its clearer seismic expression). The root zone of the pipes, at the time of their generation, was likely situated at horizons K90-K80 therefore within a range of burial depths and temperature which could have led to the generation of biogenic gas. b) RMS amplitude map extraction at T10 horizon (red: high amplitudes, grey: low amplitudes), with superimposed the modelled area of biogenic gas productivity during the late Paleocene (green colour). The extent of the pipe province mapped on the 3D dataset is spatially coincident with the modelled area of biogenic gas productivity, pointing to a causal link between pipes formation and biogenic gas generation in the Paleocene.

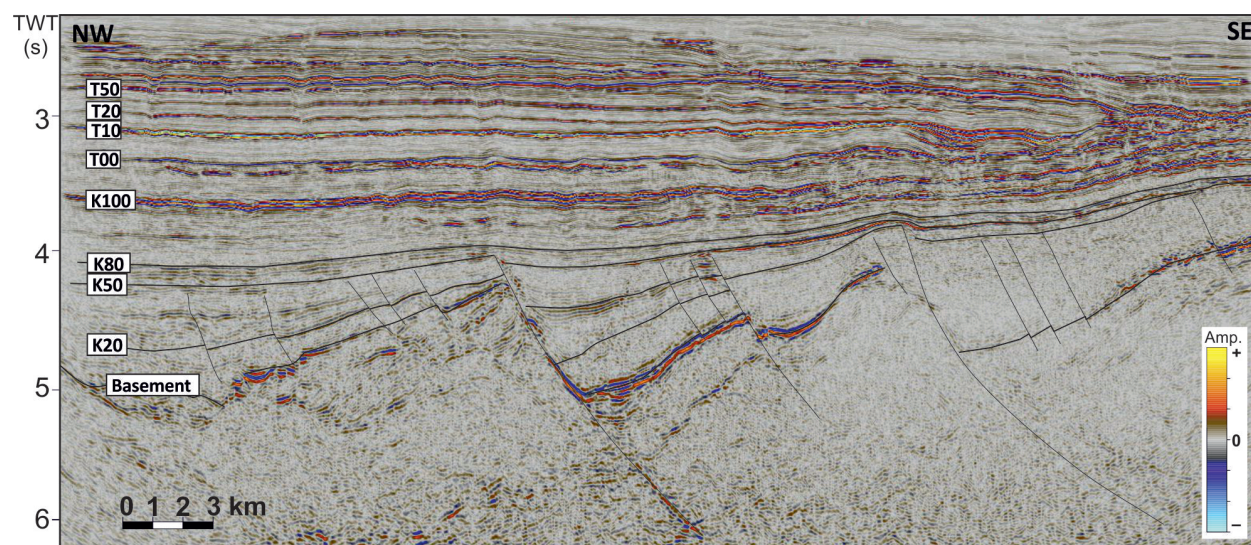


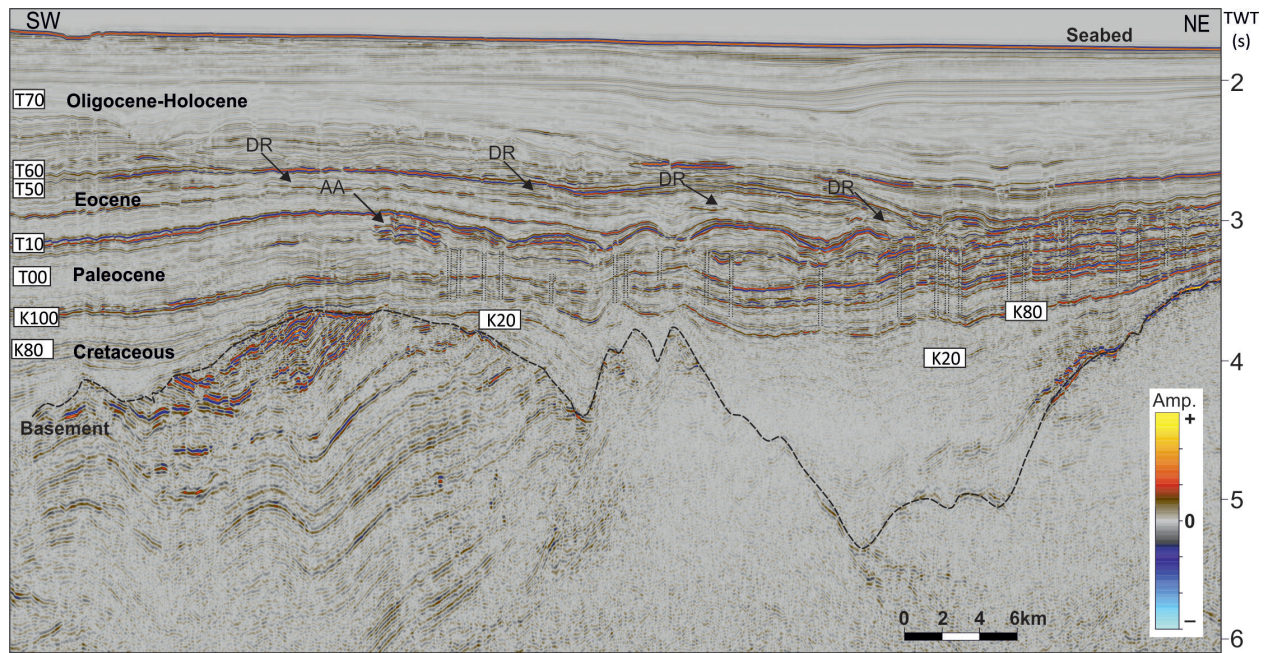


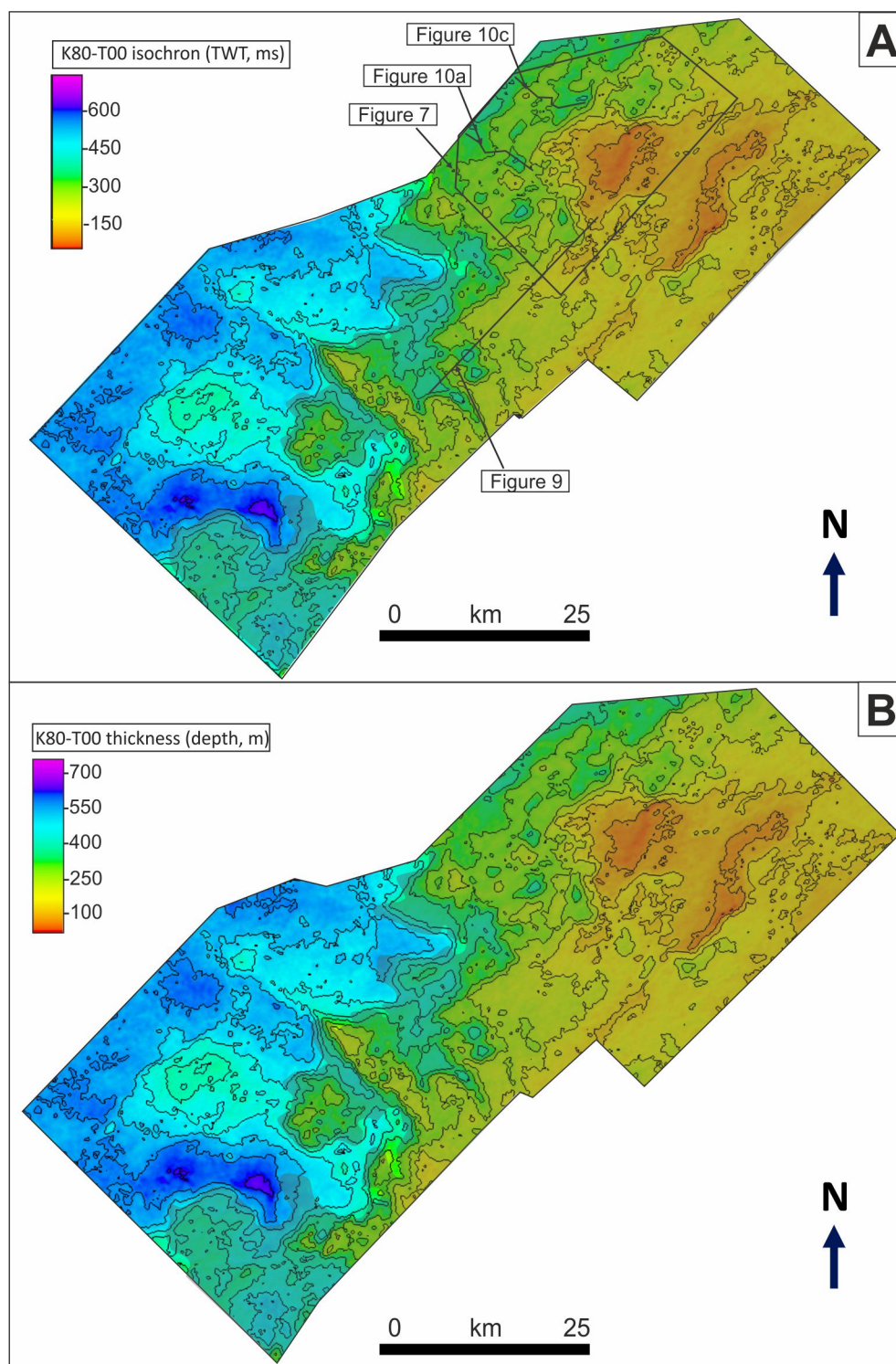


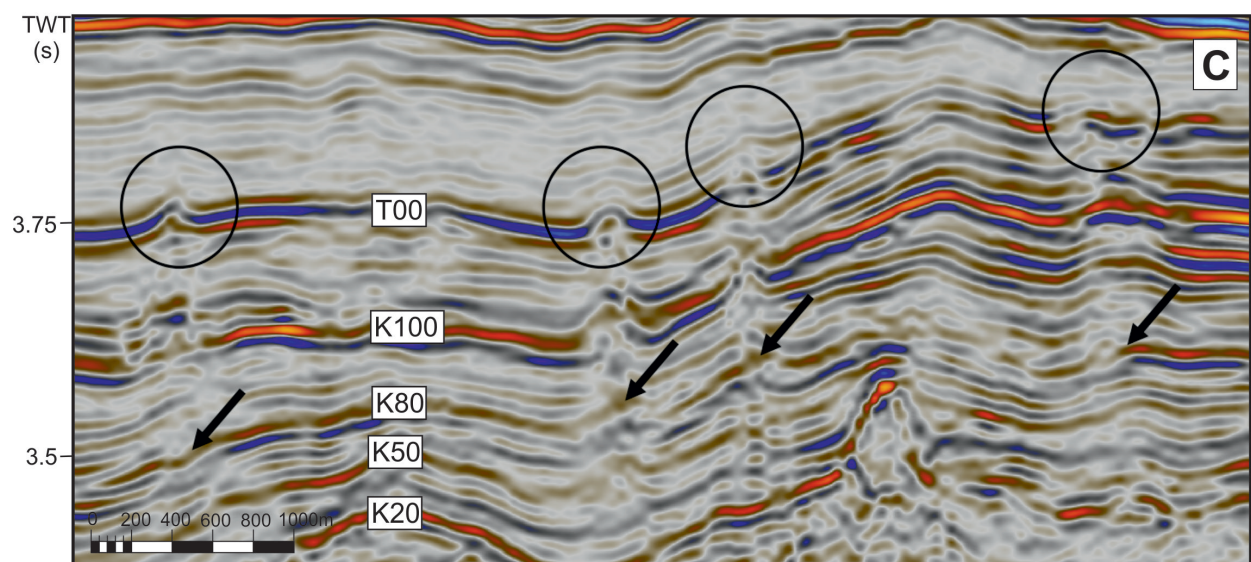
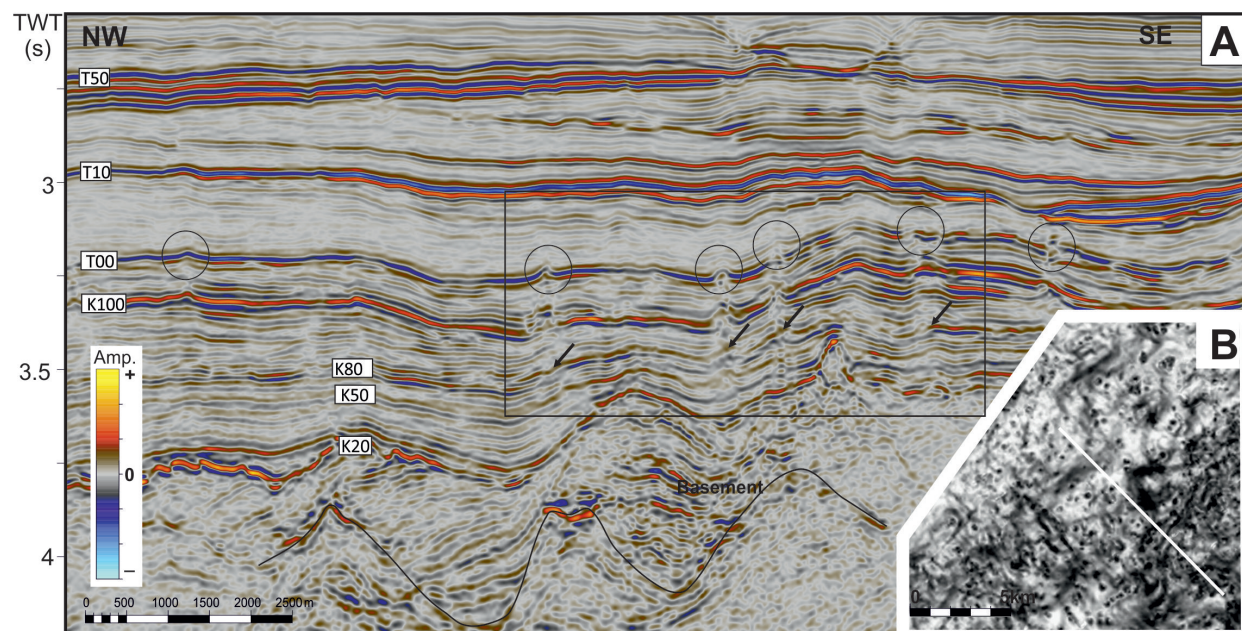


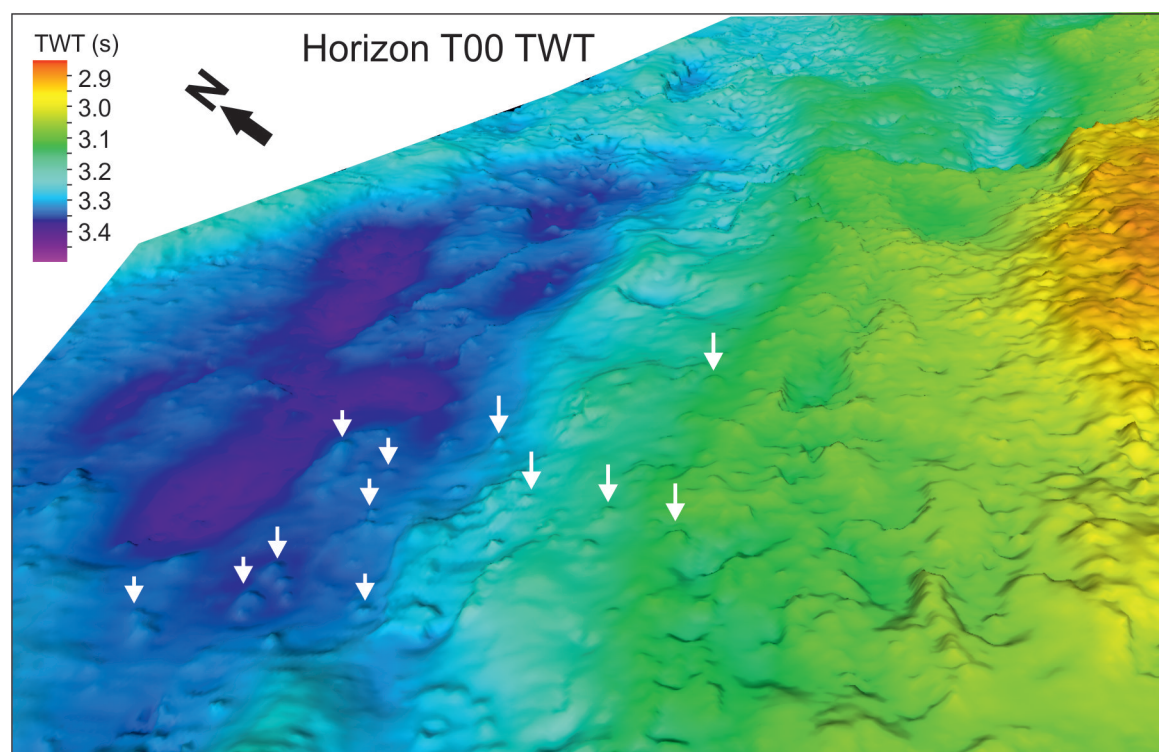


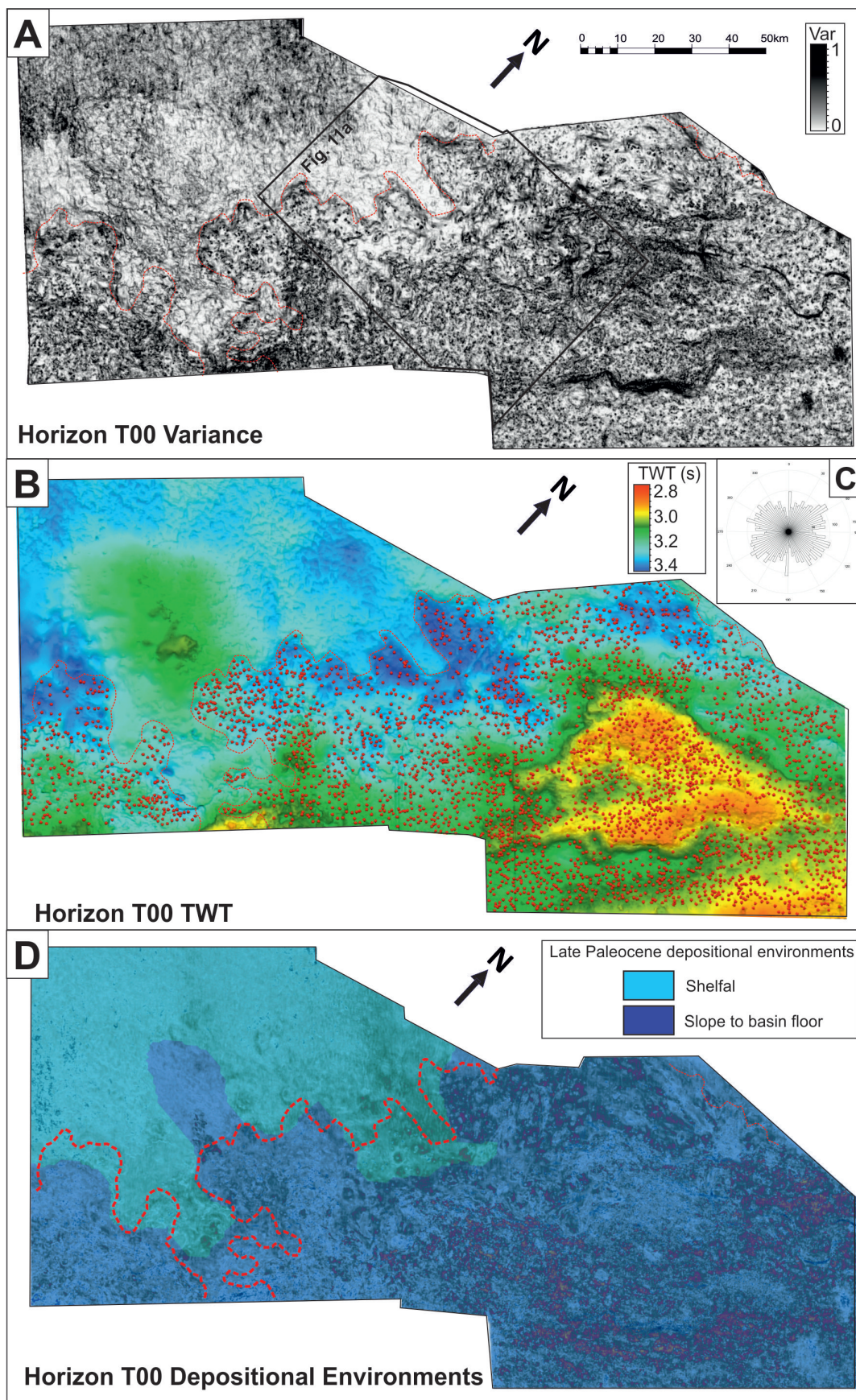


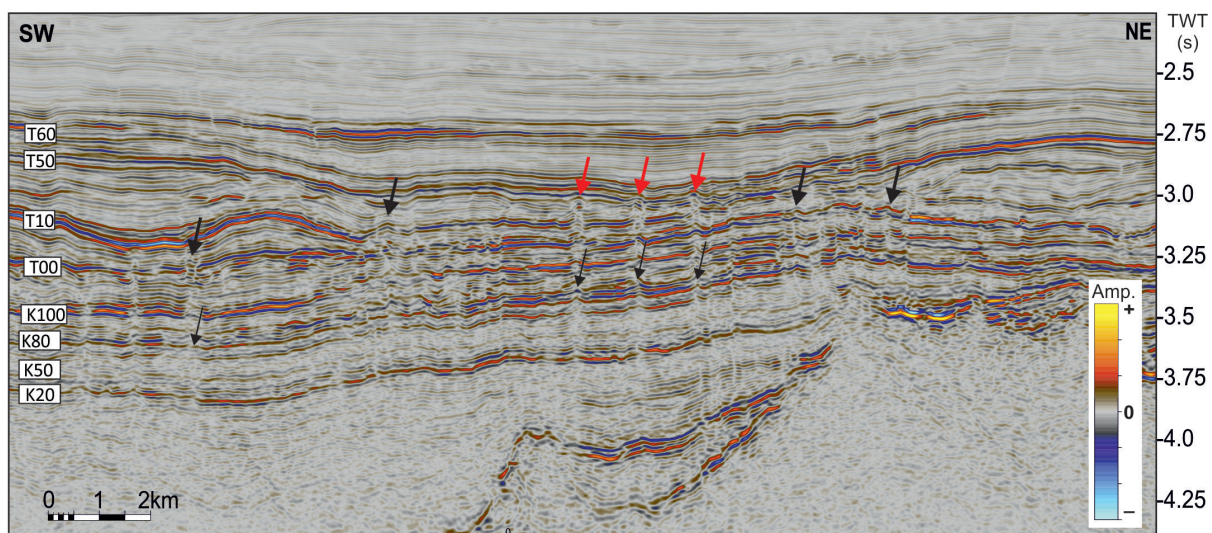












- Unusually vast fossil system of fluid escape pipes discovered offshore New Zealand
- The >2000 pipe edifices formed in the late Paleocene and are at present deeply buried
- They are associated to overpressure development linked to biogenic gas generation
- Gas release likely associated with late Paleocene Carbon Isotope Maximum sea-level fall